MIMO FSO COMMUNICATION USING HYBRID SUBCARRIER INTENSITY MODULATION OVER DOUBLE GENERALIZED GAMMA FADING

submitted in partially fulfilment of the requirements for the degree of

Bachelor of Technology

in

Electronics and Communication Engineering

by

Jaivardhan Sharma (1609731038)

Jayesh Kumar (1609731041)

Krishn Gopal Dwivedi (1609731047)

Honey Singh (1609731036)

Under the Guidance of

Mr. Piyush Jain

Associate Professor

Department of Electronics and Communication Engineering

(*B. Tech ECE - Accredited by NBA*)

Galgotias College of Engineering and Technology, Greater Noida.

(Affiliated to Dr. A.P.J. Abdul Kalam Technical University, Lucknow)

April, 2020

DECLARATION

We hereby declare that the thesis entitled **“MIMO FSO Communication using hybrid subcarrier intensity modulation over double generalized gamma fading”** submitted by us, for the award of the degree of *Bachelor of Technology in Electronics and Communication Engineering* to Galgotias College of Engineering and Technology, Greater Noida affiliated to Dr. A.P.J. Abdul Kalam Technical University, Lucknow is a record of bonafide work carried out by us under the supervision of Mr. Piyush Jain.

We further declare that the work reported in this thesis has not been submitted and will not be submitted, either in part or in full, for the award of any other degree or diploma in this institute or any other institute or university.

Place : Greater Noida

Date : **Signature of the Candidates**

CERTIFICATE

This is to certify that the thesis entitled **"MIMO FSO Communication using hybrid subcarrier intensity modulation over double generalized gamma fading"** submitted by Jaivardhan Sharma, Krishn Gopal Dwivedi, Jayesh Kumar and Honey Singh, Department of Electronics and Communication Engineering, Galgotias College of Engineering and Technology, Greater Noida affiliated to Dr. A.P.J. Abdul Kalam Technical University (AKTU), Lucknow, for the award of the degree of *Bachelor of Technology in Electronics and Communication Engineering*, is a record of bonafide work carried out by him under my supervision, as per AKTU code of academic and research ethics.

The contents of this report have not been submitted and will not be submitted either in part or in full, for the award of any other degree or diploma in this institute or any other institute or university. The thesis fulfils the requirements and regulations of the University and in my opinion meets the necessary standards for submission.

Place : Greater Noida

Date :

Signature of the Guide

The thesis is satisfactory / unsatisfactory

Internal Examiner **External Examiner**

Approved by

Head of the Department

ABSTRACT

FSO is a line-of-sight technology that uses lasers to provide optical bandwidth connections or FSO is an optical communication technique that propagate the light in free space means air, outer space, vacuum, or something similar to wirelessly transmit data for telecommunication and computer networking. One of the major limitations of FSO is the atmospheric turbulence which leads to increase in BER and degradation of intensity of signals resulting in degradation of system performance. For this reason, many channel models have been formerly proposed according to different turbulence conditions for example; lognormal, gamma-gamma, negative exponential model, etc. Modulation techniques are also used for achieving high data rates and low BER. In this thesis, symbol error rate is calculated for MIMO FSO system for different modulation techniques such as MPAM and MQAM. Graphs are plotted for BER vs SNR for different turbulence conditions using different modulation techniques. Analysis is made on the basis of simulation results.

ACKNOWLEDGEMENT

First of all, we would like to express our gratitude to our beloved **Chairman Shri. Suneel Galgotia and CEO Shri. Dhruv Galgotia** for proving necessary facilities to carry out and finish the project successfully. We are grateful to our **Director Dr. V.K. Dwivedi** for his support and encouragement.

Our special thank goes to **Dr. Lakshmanan. M, Head of the Department, Electronics and Communication Engineering,** for providing an environment that encouraged us for working towards our goal and supported in completion of our project. This project gave us an opportunity to apply creative and critical thinking skills.

We would like to present our deep sense of gratitude to our project guide, **Mr. Piyush Jain Associate Professor, Department of Electronics and Communication Engineering** who has always been a source of motivation and firm support for carrying out the project. The supervision and support that he gave truly helped in the progression of the project. His cooperation is much indeed appreciated. We are highly obliged to him for his valuable advices and moral support during research period.

Finally, our greatest and special gratitude goes to our family for their love and support.

Place: Greater Noida
Date:

Jaivardhan Sharma
Jayesh Kumar
Krishn Gopal Dwivedi
Honey Singh

Chapter No.	CONTENTS	Page No.

LIST OF FIGURES

LIST OF TABLES

CHAPTER 1

INTRODUCTION

Free Space Optics (FSO) is an optical communication technology which has emerged as a boon in the field of wireless communication. It has been the center of research activities from past few years as it is being considered as an ultimate solution for the last mile problem. In recent years, the increasing demands of larger bandwidth and less power requirements have become a reason for preferring FSO over RF. As new advances are made in optics and communication devices, there has been a renewed, increasing interest in analyzing and enhancing wireless optical links and adopting FSO technology for wireless access networks. FSO is a flexible network having advantages like high transmission rates, unlicensed spectrum, immunity to electromagnetic interference, high security and many more which has extended its usage to a wide variety of applications [4]. FSO communication link is currently in use for many services at many places. Working of FSO is similar to OFC (optical fibre cable) networks but the only difference is that the optical beams are sent through free air instead of OFC cores that is glass fibre. FSO system consists of an optical transceiver at both ends to provide full duplex capability. Free-space point-to-point optical links can be implemented using infrared laser light, although low-data-rate communication over short distances is possible using LEDs. FSO communication is not a new technology. It has been in existence from 8th century but now is more evolved. FSO is a LOS (line of sight) technology, where data, voice, and video communication can be achieved. for FSO offers many advantages over existing techniques which can be either optical or radio or microwave. Optical equipment can be used in FSO system with some modification. The transmission in FSO is dependent on the medium because the presence of foreign elements like rain, fog, and haze, physical obstruction, scattering, and atmospheric turbulence are some of these factors. One of the major limiting factors of FSO communication is the atmospheric turbulence which is caused due to the inhomogeneities in temperature and pressure resulting in random fluctuations in refractive index of air [2]. The atmospheric turbulence leads to increase in bit error rate and also degrades the intensity of signal. Although pre study of the medium can guide what type of parameters should be considered before setting up the system. Also, many statistical models have been proposed formerly, considering the intensity of modulation from weak to moderate to strong. Modulation techniques are also used so as to reduce the effect of atmospheric turbulence. Many more research activities are currently going on in this field to develop a better system.

1.1 HISTORY

The idea of wireless communication technology is present between us from early times. Early experiments in FSO included demonstrations by Alexander Graham Bell, which preceded his invention of the telephone. Bell used beams of light to transmit voice conversations through the air, which he dubbed the ‘photophone’. Though Bell’s experiment never translated into a commercial device, the principle of FSO was proved. In 1880, Alexander Graham Bell and his assistant Charles Sumner Tainter created the photophone, at Bell’s newly established Volta Laboratory in Washington, DC. The device allowed for the transmission of sound on a beam of light. On June 3, 1880, Bell conducted the world’s first wireless telephone transmission between two buildings, some 213 meters (700 feet) apart.

The first practical use of this technology came in military communication systems many decades later, first for optical telegraphy. German colonial troops used heliograph telegraphy transmitters during the Herero and Namaqua genocide starting in 1904, in German South-West Africa (today’s Namibia) as did British, French, US or Ottoman signals. During World War I when wire communications were often cut, German signals used three types of optical Morse transmitters called *Blinkgerät*, the intermediate type for distances of up to 4 km (2.5 miles) at daylight and of up to 8 km (5 miles) at night, using red filters for undetected communications. Optical telephone communications were tested at the end of the war, but not introduced at troop level. In addition, special blinkgeräts were used for communication with airplanes, balloons, and tanks, with varying success. More recently, free space optics has long been used by the military and space agencies such as NASA to provide high-speed wireless communications using non-radio media, including between satellites, drones and other vehicles.

1.2 WORKING OF FSO

Wireless optical communication (WOC) is classified as indoor and outdoor wireless optical communication. Indoor WOC ranges from 750 nm to 950 nm which is IR whereas outdoor WOC is known as free space optical communication [29]. In FSO the transmitter LED or laser diode is at the transmitter end sends the data like video images, data files through the unguided light beam in free space rather than an optical fibre. At the receiver end these beams of lights are captured by the receiving lens connected to the highly sensitive receiver [90]. Optical carrier operating in IR wavelength is used to establish connection between the terrestrial links within the earth and between inter satellite (space optical links).

Unlike radio frequencies, this technology requires no spectrum licenses. It is easily upgradable, and its open interfaces support equipment from a variety of vendors, which helps carriers protect the investment in their embedded infrastructures.

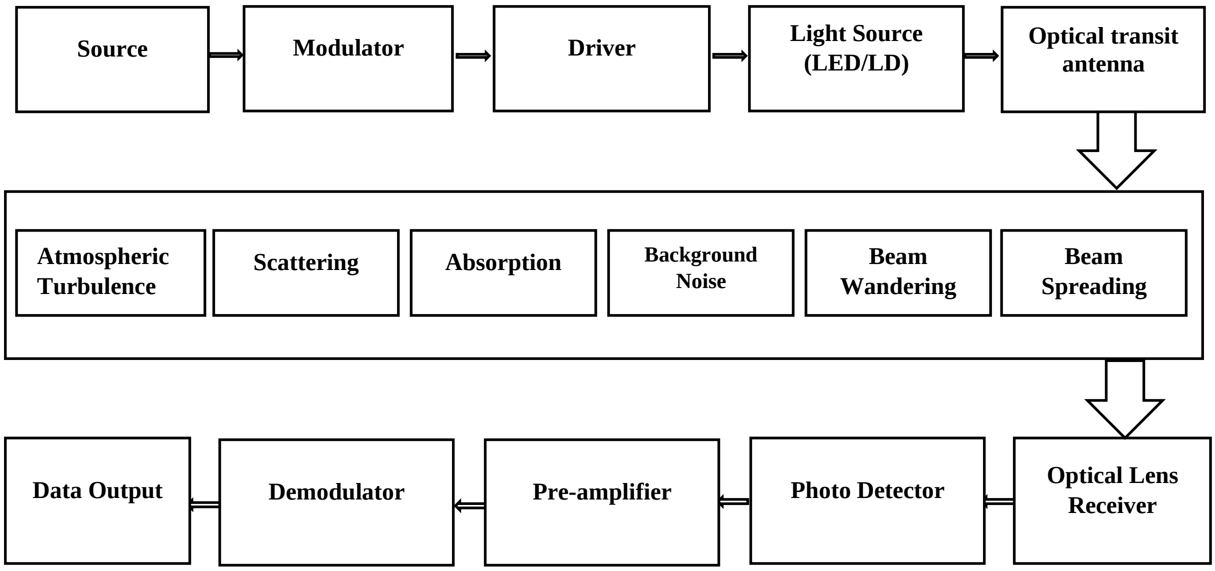

Fig.1.1 Block diagram of FSO Communication System [29]

Its working is similar to optical fibre cable. But, in FSO the optical beams are sent though free air instead of glass fibre. It works on the basis of line of sight technology and can function over distances of several kilometres as long as there is clear line of sight between the source and the destination.

1.3 APPLICATIONS

FSO communication link is currently in use for many services at many places. These are described below in detail:

1.3.1 Outdoor wireless access: It can be used by wireless service providers for communication and it requires no license to use the FSO as it is required in case of microwave bands.

1.3.2 Storage Area Network (SAN): FSO links can be used to form a SAN. It is a network which is known to provide access to consolidated, block level data storage.

1.3.3 Last-mile access: to lay cables of users in the last mile is very costly for service providers as the cost of digging to lay fibre is so high and it would make sense to lay as much fibre as possible. FSO can be used to solve such problem by implementing it in the last mile along with other networks. It is a high-speed link. It is also used to bypass local-loop systems of other kinds of networks [27].

1.3.4 Enterprise connectivity: FSO systems are easily installable. This feature makes it applicable for interconnecting LAN segments to connect two buildings or other property [27].

1.3.5 Fibre backup: FSO can also be applicable in providing a backup link in case of failure of transmission through fibre link.

1.3.6 Backhaul: it can be helpful in carrying the traffic of cellular telephone from antenna towers back to the PSTN with high speed and high data rate. The speed of transmission would increase [28].

1.3.7 Service acceleration: it can also be used to provide instant service to customers when their fibre infrastructure is being deployed in the meantime.

1.3.8 Video surveillance and monitoring: Surveillance cameras are widely deployed in commercial, law enforcement, public safety, and military applications. Wireless video is convenient and easy to deploy, but conventional wireless technologies fail to provide high throughput requirements for video streams. FSO technology presents a powerful alternative to support high quality video transmission [28].

1.3.9 Point-to-point links: It can be used to communicate between point-to-point links, for example, two buildings, two ships, and point-to-multipoint links, for example, from aircraft to ground or satellite to ground, for short and long reach communication [27].yahan ayega

1.3.10 Military access: as it is a secure and undetectable system it can connect large areas safely with minimal planning and deployment time and is hence suitable for military applications [27].

1.4 ADVANTAGES OF FSO

Free Space Optical communication has various advantages over the Radio Frequency communication. The RF wavelength is larger than the Optical wavelength. This wavelength difference shows FSO is more advantageous than RF [29].

1.4.1 LARGE BANDWIDTH

Increase in the carrier frequency causes increase in high data rate transmission. In Optical communication the optical carrier frequency is high when compared with the RF communication.

1.4.2 LESS POWER REQUIREMENT

Because of narrow beam divergence, the optical intensity of the transmitted beam power is more at the receiver than the RF. Smaller wavelength of the FSO leads to the reduction in the size of antenna when compared with the RF [29].

1.4.3 UNLICENCED SPECTRUM

Spectrum licensing is the main difference between RF and FSO. FSO requires no spectrum licensing which leads to easy and cost-effective deployment. RF requires spectrum licensing to avoid the interference. FSO requires line of sight communication.

1.4.4 HIGH SECURITY

Optical beam cannot penetrate the walls so information transfer is secure. FSO beams cannot be detected using a spectrum analyser as in case of RF [29].

The other advantages of FSO are listed below:

1. Free space optics is a flexible network that delivers better speed than broadband.
2. Easy installation.
3. Low initial investment
4. Immunity to radio frequency interference.
5. Electromagnetic and radio-magnetic interference cannot affect the transmission in FSO link
6. FSO offers dense spatial reuse.
7. Low power usage per transmitted bit is merit of FSO system.
8. It has flexible rollouts.

1.5 CHALLENGES FACED IN FSO

In Free Space Optical communication, the optical wave is propagating in free space is subjected to many disturbances. The disturbances like absorption, scattering and turbulence cause the attenuation of the wave. The electromagnetic properties, shape and direction of the beam are affected by these disturbances which in turn affects the overall performance of the optical link. FSO link distance is dependent on the unpredictable weather conditions like fog, rain and haze [29].

1.5.1 FSO TERRESTIAL LINKS

In FSO Terrestrial links the communication is within the Earth's surface either from building to building or between two stations. The connection between the points may be point to point, point to multipoint. When the optical beam is propagating between two points in free space the transmitted beam is affected by various factors such as beam divergence, atmospheric losses, atmospheric turbulence and ambient light.

1.5.1.1 Beam Divergence: The diffraction at the aperture end of the transmitter telescope causes beam divergence. The amount of signal energy collected by the receiver is determined by the divergence. FSO transmitted beam is diffracted from the limit which causes losses like geometric loss and misalignment loss. The divergence angle of the transmitted optical beam should match with the field of view of receiver telescope [30]. Misalignment losses are caused by building sway. To reduce the losses due to beam divergence, the aperture size of the receiver lens has to be adjusted according to beam divergence angle.

1.5.2 ATMOSPHERIC LOSSES

The attenuation in the optical beam called atmospheric losses is caused by absorption and scattering of beam. The atmospheric loss is given by Beer's law. Absorption is the reduction in the signal energy of the beam by the absorption of energy by the particles present in the atmosphere. The absorbing particles are divided as molecular and aerosol absorbers [31]. Molecular absorption is due to the gases present in the atmosphere which are N_2, H_2 etc. Aerosols are the suspended particles in the medium. The liquid particles present in atmosphere are in the form of mist, fog. The solid particles are dust, volcanic particles, etc. Scattering occurs when light collides with the particles present in the medium which leads to the redistribution of light or deflection in the angle of arrival. Scattering and absorption are wavelength dependent. When the size of the colliding particle is less than the wavelength of the beam then it is called as Rayleigh scattering. When the particle size is comparable of the wavelength then it is called as Mie scattering. When the particle size is larger than the wavelength of the beam then it is non selective scattering [32]. The atmospheric factors which cause scattering and absorption are fog, rain, snow and sand.

1.5.2.1 Fog: Fog is the main challenge for FSO communication since it causes both scattering and absorption. The density of the fog varies based on the particle size. It is classified as thin fog, light fog, moderate fog and thick fog. The density of the fog varies with the height which makes the modelling complex. The communication link is difficult to maintain under dense fog condition which results in switching the link to RF. By increasing the transmitting power, the performance of the system can be improved under light fog condition. By using multi-hop link, the power budget of the system can be improved under the low visible range. The bit error rate of $10^{-3}$is obtained for the distance of 1 km in light fog, but under dense fog, same bit error rate occurs at distance of 200 m link length [33].

1.5.2.2 Rain: Rain is another reason for attenuation of the signal in FSO Communication. The radius of the raindrop is larger than the wavelength of the FSO source. Heavy rain can lead to the link failure. But the effect of attenuation of the rain is low when compared with the fog. For frequencies less than 10 GHz, specific attenuation due to rain is less. Rain is the main attenuation factor for RF link when the frequency is above 10 GHz. For frequencies higher than 40 GHz, the attenuations are more for RF links [34]. Hybrid RF/FSO provides better link availability under various weather conditions. If link availability is a major consideration then RF link below 10 GHz is considered as the best choice of backup link. If data rate as the major consideration compromising the link availability then RF link below 40 GHz is considered as the best choice.

1.5.2.3 Snow: Snow has droplet size between rain and fog. The attenuation effect of snow is between rain and fog. The size of the snowflakes blocks the laser light [29].

1.5.2.4 Sand: Sand particles also cause scattering effect. In deserts sand particles reduces the link availability [29].

1.5.3 ATMOSPHERIC TURBULENCE

The variation in the temperature and pressure of the air sets a random phenomenon called Atmospheric turbulence. Due to the variation in the refractive index, the atmosphere acts like different cells called eddies. These eddies deflect the light transmission path. The turbulence is measured in terms of refractive index structure coefficient C_n^2. The C_n^2 value varies depending on the time of the day. The laser beam undergoes three atmospheric turbulence effects. They are Scintillation, beam wandering and beam spreading [30].

1.5.3.1 Scintillation: The random fluctuation in the air sets a fluctuation in the intensity of the propagating wave. The intensity of the fluctuating wave is measured in terms of scintillation index. The strength of the atmospheric turbulence is classified on the scintillation index [29].

1.5.3.2 Beam Wandering: When the size of the refractive indices of the cells exceeds the beam size then random fluctuation occurs in the beam which results in deflection in the direction of propagation of the beam. Beam wandering affect the signal quality. Beam wandering increases with the distance.

1.5.3.3 Beam Spreading: Beam spreading is the spread of the propagating optical beam in the atmosphere. Beam spreading is reduced by increasing the average aperture radius. It occurs when the beam is diffracted near the receiver aperture. Beam spreading due to atmospheric turbulence occurs when the size of the beam is larger than the size of the eddy cells.

1.5.3.4 Ambient Light: Ambient light sources like sun, moon and fluorescent light are the main causes of background noise. These noises are modelled as white, Gaussian and signal independent noise. These noises are added to the detector noise. Background noises area modelled by Poisson random variables. It is advantageous to select the wave- length of the optical beam longer than the wavelength of telecom of 1.5lm. Selection of higher wavelengths reduces the background radiations. The effect of background noise is reduced by using double wavelength transmission and differential mode data detection methods [35].

1.6 MODULATION TECHNIQUES

A modulation technique which offers high transmission rate and low bit error rate can be used to reduce the effect of atmospheric turbulence. Various modulation techniques such as PPM, BPSK and OOK have been analysed and the outcome is that PPM has poor bandwidth efficiency, BPSK is mostly used as it gives the lowest BER, OOK is simple to implement but it is found to be suboptimal over atmospheric turbulence channel [3]. SIM is used as an alternative to OOK and it is studied over the years that

BPSK SIM is better than the other modulation techniques such as QPSK, MPSK and so on.

1.6.1 TYPES OF MODULATION

Modulation is the process of varying message signal in accordance with the carrier signal. Modulation can be analog as well as digital in nature. Modulation is required as it helps to reduce the size of antenna, reduces noise, allows intermixing mixing of signal and long-distance transmission. Digital communication has achieved the great attention. There are various modulation techniques discussed below.

1.6.1.1 BPSK: The most straightforward type of PSK is called binary phase shift keying (BPSK), where “binary” refers to the use of two-phase offsets (one for logic high, one for logic low) where the 0’s and 1’s in a binary message are represented by two different phase states in the carrier signal: $\theta=0^\circ$ for binary 1 and $\theta=180^\circ$ for binary 0.

1.6.1.2 MPSK: In M-ary or multiple phase-shift keying (MPSK), there are more than two phases, usually four (0, +90, -90, and 180 degrees) or eight (0, +45, -45, +90, -90, +135, -135, and 180 degrees). If there are four phases (m = 4), the MPSK mode is called quadrature phase-shift keying or quaternary phase-shift keying (QPSK), and each phase shift represents two signal elements. If there are eight phases (m = 8), the MPSK mode is known as octal phase-shift keying (OPSK), and each phase shift represents three signal elements. In MPSK, data can be transmitted at a faster rate, relative to the number of phase changes per unit time, than is the case in BPSK. It is a modulation technique where data bits select one of M phase shifted versions of the carrier to transmit the data. Thus, the M possible waveforms all have the same amplitude and frequency but different phases. The signal constellations consist of M equally spaced points on a circle.

1.6.1.3 QPSK: In MPSK modulation if there are four phases (m = 4), the MPSK mode is called quadrature phase-shift keying or quaternary phase-shift keying (QPSK), and each phase shift represents two signal elements. In this, two bits are modulated at once, selecting one of four possible carrier phase shifts (0, 90, 180, or 270 degrees). QPSK allows the signal to carry twice as much information as ordinary PSK using the same bandwidth.

1.6.1.4 DPSK: The phase of the modulated signal is shifted relative to the previous signal element. No reference signal is considered here. The signal phase follows the high or low state of the previous element. This DPSK technique doesn’t need a reference oscillator. DPSK encodes two distinct signals, i.e., the carrier and the modulating signal with 180° phase shift each. The serial data input is given to the XNOR gate and the output is again fed back to the other input through 1-bit delay. The output of the XNOR gate along with the carrier signal is given to the balance modulator, to produce the DPSK modulated signal.

1.6.1.5 PAM: Pulse amplitude modulation is a technique in which the amplitude of each pulse is controlled by the instantaneous amplitude of the modulation signal. It is a modulation system in which the signal is sampled at regular intervals and each sample is made proportional to the amplitude of the signal at the instant of sampling. This technique transmits the data by encoding in the amplitude of a series of signal pulses.

1.6.1.6 QAM: Quadrature Amplitude Modulation, QAM utilises both amplitude and phase components to provide a form of modulation that is able to provide high levels of spectrum usage efficiency. Quadrature Amplitude Modulation, QAM is a signal in which two carriers shifted in phase by 90 degrees (i.e. sine and cosine) are modulated and combined. As a result of their 90° phase difference they are in quadrature and this gives rise to the name. Often one signal is called the In-phase or “I” signal, and the other is the quadrature or “Q” signal.

The resultant overall signal consisting of the combination of both I and Q carriers contains of both amplitude and phase variations. In view of the fact that both amplitude and phase variations are present it may also be considered as a mixture of amplitude and phase modulation. QAM has been used for some analogue transmissions including AM stereo transmissions, but it is for data applications where it has come into its own. It is able to provide a highly effective form of modulation for data and as such it is used in everything from cellular phones to Wi-Fi and almost every other form of high-speed data communications system.

1.6.1.7 MSK: It is a type of continuous phase shift keying that is encoded with bits alternating between quadrature components with the Q component delayed by half the symbol period.

1.6.1.8 SIM: It is a modulation technique for optical wireless communication systems, where a pre-modulated and properly biased radio frequency signal is modulated on the intensity of the optical carrier. It is a technique borrowed from the very successful multiple carrier radio frequency (RF) communications already deployed in applications such as digital television; local area networks (LANs), asymmetric digital subscriber line (ADSL), 4G communication systems and optical fibre communications. In optical fibre communication networks for example, the subcarrier modulation techniques have been commercially adopted in transmitting cable television signals and have also been used in conjunction with wavelength division multiplexing. For the seamless integration of FSO systems into present and future networks, which already harbour subcarrier modulated (or multiple carrier) signals, the study of subcarrier modulated FSO is thus imperative. Other reasons for studying the subcarrier intensity modulated FSO systems include:

1. It benefits from already developed and evolved RF communication components such as stable oscillators and narrow filters.

2. It avoids the need for an adaptive threshold required by optimum performing OOK modulated FSO.

3. It can be used to increase capacity by accommodating data from different users on different subcarriers.

4. It has comparatively lower bandwidth requirement than the PPM.

1.6.1.9 PPM: It is a form of signal modulation in which M message bits are encoded by transmitting a single pulse in one of possible required time shifts. This is repeated every T second, such that the transmitted bit rate is bits per second. This modulation technique improves on the power efficiency of OOK but at the expense of an increased bandwidth requirement and greater complexity.

In PPM, each block of $\log_2 M$ data bits is mapped to one of M possible symbols. Generally, the notation M-PPM is used to indicate the order. Each symbol consists of a pulse of constant power, P_T, occupying one slot, along with M-1 empty slots. The position of the pulse corresponds to the decimal value of the $\log_2 M$ data bits. Hence, the information is encoded by the position of the pulse within the symbol.

A PPM receiver will require both slot and symbol synchronisation in order to demodulate the information encoded on the pulse position. Nevertheless, because of its superior power efficiency, PPM is an attractive modulation technique for optical wireless communication systems particularly in deep space laser communication applications.

Table 1.1 Comments on different modulation techniques [28]

MODULATION	COMMENT
OOK	Needs dynamic thresholding at receiver
PPM	Optimal in terms of energy efficiency

MPPM	Lower PAPR and more bandwidth efficient than PPM
PWM	Needs lower peak power, better spectral efficiency, more resistant to ISI than PPM
PPMPWM	Power and bandwidth efficiencies in mid-way between PPM and PWM
DPPM	Simpler symbol synchronization and improved bandwidth efficiency than MPPM
OPPM	More bandwidth efficient than PPM
MPAM	Higher bandwidth efficiency than PPM; requires dynamic thresholding at receiver
SIM	High capacity, cost effective implementation; low power efficiency

1.7 CHANNEL MODELS

The atmospheric turbulence leads to increase in bit error rate and also degrades the intensity of signal. For this reason, many statistical models have been proposed formerly, considering the intensity of modulation from weak to moderate to strong such as lognormal, gamma-gamma, negative exponential, double Weibull, double generalized gamma model and so on.

Table 1.2 Channel models for different turbulence conditions [29]

WEAK TURBULENCE	MODERATE TURBULENCE	STRONG TURBULENCE
Log Normal Distribution	Log Normal Distribution	G-G Distribution
G-G Distribution	Negative Exponential	K-Distribution
I-K-Distribution	G-G Distribution	I-K-Distribution
I-K-Distribution	Double Weibull	Double Weibull
Exponentiated Weibull	Exponentiated Weibull	Exponentiated Weibull
Double Generalised Distribution	Double Generalised Distribution	Double Generalised Distribution

1.8 SYSTEM MODEL

The system model mainly consists of three parts:

1. Transmitter
2. Channel
3. Receiver

In general SIM based FSO technique; the information modulates the RF subcarrier signal using any specific electrical modulation technique. The intensity of the optical source is modulated by the resultant electrical modulated signal. In receiver section, the received optical signal is converted to electrical signal by a photodetector in direct detection process. Then it is followed by a normal RF coherent demodulation technique for the recovery of the original information.

1.8.1 TRANSMITTER

First, a block of M ¼ $\log_2 L$ data bits is converted into the symbol format of PPM, here, M is the number of bits per symbol or the modulation order, and L is the average length of symbol. The configuration of PPM-MSK-SIM/FSO communication systems is shown in Fig.

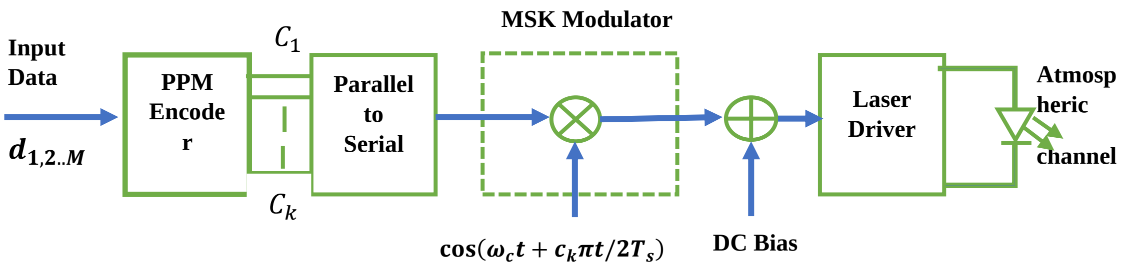

Fig.1.2 Block Diagram of FSO transmitter [3]

Conversion, finally the new array of data is modulated into the subcarrier signal using the MSK signal.

Since the modulated subcarrier signal is sinusoidal having both positive and negative values, a DC bias is added to the MSK signal 0before it is used to drive the laser diode. This can ensure that the bias current is always equal to or greater than the threshold current.

1.8.1.1 Parts of Transmitter Section: The various parts of the transmitter are discussed below:

1. PPM Encoder: PPM Encoder allows to encode up to 8 Pulse Width modulated signal into 1 PPM. As we know, PPM is a form of signal modulation in which M message bits are encoded by transmitting a single pulse in one of possible required time shifts. This is repeated every T second, such that the transmitted bit rate is bits per second. This modulation technique improves on the power efficiency of OOK but at the expense of an increased bandwidth requirement and greater complexity.

In PPM, each block of log2M data bits is mapped to one of M possible symbols. Generally, the notation M-PPM is used to indicate the order. Each symbol consists of a pulse of constant power, PT, occupying one slot, along with M-1 empty slots. The position of the pulse corresponds to the decimal value of the log2M data bits. Hence, the information is encoded by the position of the pulse within the symbol.

2. Parallel to Serial Converter: Conversion of stream of multiple data elements received simultaneously into a stream of data elements transmitted in time sequence such that it is one at a time A conversion process in which stream of information elements received all at once is converted and is sent as stream of information at one bit at a time.

3. MSK Modulator: MSK is a type of continuous phase frequency shift keying. MSK is encoded with bits alternating between quadrature components with Q components delayed by half the symbol period. MSK encodes each bit as a half sinusoid. MSK offers advantages in terms of spectral efficiency and it also enables power amplifier to operate in saturation enabling them to provide high levels of efficiency.

4. Multiplexer: It is a device that selects between several analog or digital input signals and forwards it to a single output line. A multiplexer of 2n {\displaystyle 2^{n}} inputs has {\displaystyle n}n select lines, which are used to select which input line to send to the output. A multiplexer is also called a data selector. Multiplexers can also be used to implement Boolean functions of multiple variables. An electronic multiplexer makes it possible for several signals to share one device or resource, for example, one A/D converter or one communication line, instead of having one device per input signal.

5. Local Oscillator: is an electronic oscillator used with a mixer to change the frequency of a signal. This frequency conversion process, also called heterodyning, produces the sum and difference frequencies from the frequency of the local oscillator and frequency of the input signal. Processing a signal at a fixed frequency gives a radio receiver improved performance. In many receivers, the function of local oscillator and mixer is combined in one stage called a "converter" - this reduces the space, cost, and power consumption by combining both functions into one active device.

6. DC Bias: When describing a periodic function in the time domain, the DC bias, DC component, DC offset, or DC coefficient is the mean amplitude of the waveform. If the mean amplitude is zero, there is no DC bias. A waveform with no DC bias is known as a DC balanced or DC free waveform.

7. Adder: An adder is a digital circuit that performs addition of numbers. In many computer and other kinds of processor adders are used in the arithmetic logic unit or ALU. They are also used in other parts of the processor, where they are used to calculate addresses, table indices, increment and decrement operators, and similar operations. In cases where two's complement or one's complement is being used to represent negative numbers, it is trivial to modify an adder into an adder-subtractor.

8. Laser Driver: Laser diode controllers or drivers are uniquely designed to drive a laser diode by providing a current instead of a voltage to the laser diode. They typically have a "soft start" to avoid damaging the laser diode while being powered on or off, transient protection, as well as a high modulation bandwidth – often 150 kHz or more – Laser diode drivers are sometimes also referred to as current drivers, current controllers or laser diode controllers and the names are used almost interchangeably. All laser diodes, also called diode lasers or semiconductor lasers, require a laser diode driver to operate.

1.8.2 CHANNEL

In FSO communication system the channel models are categorized according to the turbulence level of channels. So, the channel models are defined as log-normal model for weak turbulence, negative-exponential model for strong turbulence and gamma-gamma channel model for moderate turbulence level. Application of FSO for short distance communication in urban areas is considered and the log-normal distribution is best suited for it.

Table 1.3 Channel models with turbulence conditions [29]

CHANNEL MODEL	TURBULENCE
Log normal	Weak
Gamma-Gamma	Moderate
Negative exponential	Strong

1.8.2.1 Double Generalised Gamma Distribution: The generalized gamma distribution is a continuous probability distribution with three parameters. It is a generalization of the two-parameter gamma distribution. Since many distributions commonly used for parametric models in survival analysis (such as the Exponential distribution, the Weibull distribution and the Gamma distribution) are special cases of the generalized gamma, it is sometimes used to determine which parametric model is appropriate for a given set of data. Another example is the half-normal distribution. Double Generalised Gamma Distribution is a type of generalized gamma distribution in which the received irradiance fluctuations is assumed to be the modulation of small-scale irradiance fluctuations by large-scale irradiance fluctuations [1].

1.8.3 RECEIVER

At the receiver end, the incoming optical radiation need to be filtered firstly through an optical band pass filter (OBPF), then it is converted into electrical signal, which is

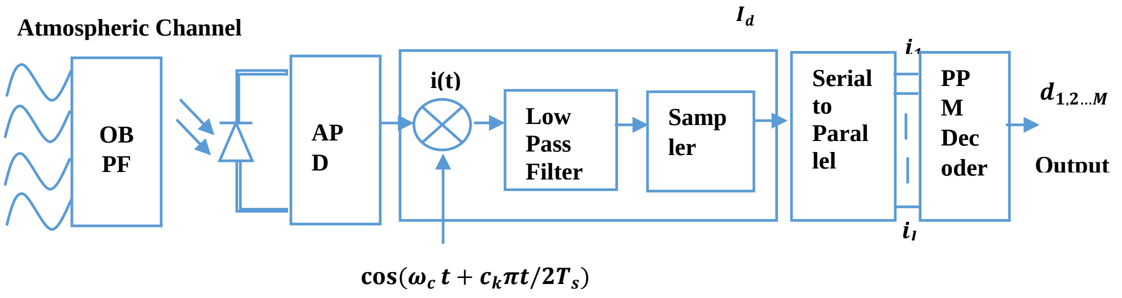

Fig.1.3 Block diagram of FSO receiver [3]

detected by an APD directly. During the propagation over atmospheric channel, the modulated optical signal's amplitude and phase are distorted by absorption and scattering from fog, clouds, rain, snow and dust. The link loss consists of geometric loss and atmospheric attenuation.

1.8.3.1 Parts of Receiver Section: The various parts of the receiver are discussed below,

1. OBPF: A band-pass filter may also be called a **band-select filter** as it selects a specific frequency range to pass a signal attenuated. This type of filter is the most frequently used. Band-pass filters may be built from all common transmission line media, ranging from waveguide to micro strip line. A basic feature of the geometry of a filter is that it may consist of resonators coupled along the transmission path of signal, and its number of poles is related to the number of resonant modes of the filter.

2. APD Photo Detector: An APD is a highly sensitive semiconductor electronic device that exploits the photoelectric effect to convert light to electricity. APDs can be thought of as photodetectors that provide a built-in first stage of gain through avalanche multiplication. From a functional standpoint, they can be regarded as the semiconductor analog of photomultipliers. By applying a high reverse bias voltage (typically 100–200 V in silicon), APDs show an internal current gain effect (around 100) due to impact ionization. However, some silicon APDs employ alternative doping and bevelling techniques compared to traditional APDs that allow greater voltage to be applied (> 1500 V) before breakdown is reached and hence a greater operating gain (> 1000). In general, the higher the reverse voltage, the higher the gain.

3. LPF: LPF is a filter that passes signals with a frequency lower than a selected cut off frequency and attenuates signals with frequencies higher than the cut-off frequency. The exact frequency response of the filter depends on the filter design. The filter is sometimes called a high-cut filter or treble-cut filter in audio applications. A low-pass filter is the complement of a high-pass filter.

Low-pass filters exist in many different forms, including electronic circuits such as a hiss filter used in audio, anti-aliasing filter for conditioning signals prior to analog to digital conversion, digital filter for smoothing sets of data, acoustic barriers, blurring of images, and so on. The moving average operation used in fields such as finance is a particular kind of low-pass filter, and can be analysed with the same signal processing techniques as are used for other low-pass filters. Low-pass filters provide a smoother form of a signal, removing the short-term fluctuations and leaving the longer-term trend.

4. Sampler: In signal processing, sampling is the reduction of a continuous time signal to a discrete time signal. A common example is the conversion of a sound wave (a continuous signal) to a sequence of samples (a discrete-time signal).A sample is a value or set of values at a point in time and/or space. A sampler is a subsystem or operation that extracts samples from a continuous signal. A theoretical ideal sampler produces samples equivalent to the instantaneous value of the continuous signal at the desired points.

5. Serial to Parallel Converter: A serial to parallel converter is a digital circuit where we feed the input data serially, and read the outputs in parallel fashion. A 4-bit serial-to-parallel shift register is one of the simplest types of circuits utilising four D-type flip-flops. Shift registers are widely in use in modern digital electronics. Data communications from a USB port or a

SATA hard disk drive are in serial, and there is usually a controller IC that converts this data into parallel before sending to the microprocessor.

6. PPM DECODER: Traditional PPM decoders use a shift register or counter to separate out the channels. PPM decoder allows decoding up to 8 Pulse Width modulated signal into 1 Pulse Position Modulation. As we know, PPM is a form of signal modulation in which M message bits are encoded by transmitting a single pulse in one of possible required time shifts. This is repeated every T second, such that the transmitted bit rate is bits per second. This modulation technique improves on the power efficiency of OOK but at the expense of an increased bandwidth requirement and greater complexity.

1.9 MOTIVATION

Modelling and analysis of hybrid SIM using LPPM MPSK combines the advantages of PPM and MPSK over double generalised gamma distribution in free space optical communication which provides unlicensed spectrum, low cost, low power consumption, better security, high data rates.

1.10 THESIS OUTLINE

In chapter 2, we have presented a literature survey which gives a brief regarding the different channel models and the different modulation techniques used. In chapter 3, we have discussed the mathematical model of work. In chapter 4, we have analysed the performance of hybrid-SIM with L-PPM MPSK over double GG distribution in terms of BER and presented the results for the same. Conclusion of the thesis and future works in this field are presented in chapter 5.

CHAPTER 2

LITERATURE REVIEW

Free Space Optical (FSO) communication enables wireless connectivity through atmosphere using laser transmitters at infrared bands. These systems provide high data rates comparable to fiber optics. Working of FSO is similar to OFC (Optical Fibre Cable) networks but the only difference is that the optical beams are sent through free air instead of OFC cores that is glass fiber. FSO system consists of an optical transceiver at both ends to provide full duplex (bidirectional) capability. FSO communication is not a new technology. It has been in existence from 8th century but now is more evolved. FSO systems have attracted attention initially as a last mile solution and can be used in a wide array of applications including cellular backhaul, inter-building connections in enterprise/campus environments, video surveillance/ monitoring, fiber back-up, redundant link in disaster recovery and relief efforts among others.

There are various literatures having different channel distributions and different modulation techniques.

S.No.	REFERENCES	FINDINGS	LIMITATIONS
1.	Yi, X., Yao, M. and Wang, X., 2017. MIMO FSO communication using subcarrier intensity modulation over double generalized gamma fading. *Optics Communications*, *382*, pp.64-72.[1]	Average symbol error rate (SER) of MPSK for SIM-based MIMO FSO systems employing RC and OSTBC schemes in terms of double power series.	BER performance of BPSK SIM is not analyzed which is better than MPSK SIM.

2.	Kashani, M.A., Uysal, M. and Kavehrad, M., 2015. A novel statistical channel model for turbulence-induced fading in free-space optical systems. *Journal of Lightwave Technology*, *33*(11), pp.2303-2312.[2]	Closed form expression for BER and outage probability of SIMO and SISO FSO system with intensity modulation and direct detection (IM/DD).	No modulation technique is employed.
3.	Liu, H., Liao, R., Wei, Z., Hou, Z. and Qiao, Y., 2015. BER analysis of a hybrid modulation scheme based on PPM and MSK subcarrier intensity modulation. *IEEE Photonics Journal*, *7*(4), pp.1-10.[3]	BER performance of PPM-MSK-SIM.	Log normal distribution is used which is applicable for weak turbulence conditions only.

A new generic fading model, called double-generalized gamma (double GG), is developed for accurately describing irradiance fading over a wide range of turbulence conditions. So, for a general and exact study of the multiple-input multiple-output (MIMO) FSO system, the double GG fading model is adopted. The MIMO FSO systems using subcarrier intensity modulation is investigated [1]. Firstly, a new power series expression is proposed for the probability density function of the double GG fading then the average error rate expressions is derived for both schemes in terms of double power series. The truncated forms of the derived power series enable the rapid and accurate numerical computation of the error rates. Furthermore, the asymptotic error rate analyses at high electrical signal-to-noise ratio (SNR) for both schemes is presented.

A new probability distribution function which accurately describes turbulence-induced fading under a wide range of turbulence conditions. The proposed model, termed Double

Generalized Gamma (Double GG), is based on a doubly stochastic theory of scintillation and developed via the product of two Generalized Gamma (GG) distributions [2]. The proposed Double GG distribution generalizes many existing turbulence channel models and provides an excellent fit to the published plane and spherical wave simulation data. Using this new statistical channel model, a closed form expression is derived for the outage probability and the average bit error as well as corresponding asymptotic expressions of free-space optical communication systems over turbulence channels in [2]. It is demonstrated that the derived expressions cover many existing results in the literature earlier reported for Gamma-Gamma, Double-Weibull and K channels as special cases.

The bit-error-rate (BER) performance of free-space optical (FSO) communication systems is improved by employing binary phase-shift keying subcarrier intensity modulation (BPSK-SIM), an innovative hybrid modulation scheme called PPM-MSK-SIM is proposed, which is based on pulse position modulation (PPM) and minimum shift keying (MSK) subcarrier intensity modulation [3]. Subsequently, the BER performance of PPM- MSK-SIM is studied in detail for an FSO system over log-normal turbulence channels with avalanche photodiode detection. The results of the numerical simulation in [3] show that PPM-MSK-SIM has the advantages of improving the BER performance compared with BPSK-SIM and PPM.

4.	Giri, R.K. and Patnaik, B., 2019. Bit error rate performance analysis of hybrid subcarrier intensity modulation-based FSO with spatial diversity in various weather conditions. *Journal of Optical Communications*, *40*(3), pp.307-314.[4]	BER performance of PPM MSK SIM is analyzed.	BER performance for MIMO system is not analyzed.

5.	AlQuwaiee, H., Ansari, I.S. and Alouini, M.S., 2016. On the maximum and minimum of double generalized gamma variates with applications to the performance of free-space optical communication systems. *IEEE Transactions on Vehicular Technology*, *65*(11), pp.8822-8831.[5]	Average bit error rate (BER) and the ergodic capacity (EC).	Weak turbulence condition is not analyzed.
6.	Kashani, M.A., Uysal, M. and Kavehrad, M., 2015, June. On the performance of MIMO FSO communications over double generalized gamma fading channels. In *2015 IEEE International Conference on Communications (ICC)* (pp. 5144-5149). IEEE.[6]	BER performance of single-input multiple-output (SIMO), multiple-input single-output (MISO) and multiple-input multiple-output (MIMO).	Weak turbulence condition is not analyzed.

The performance improvement of free space optical (FSO) communication system with spatial diversity techniques employing hybrid pulse position modulation-binary phase shift keying-subcarrier intensity modulation (PPM-BPSK-SIM) is studied in [4]. The involvement of multiple photo-detectors in diversity based FSO systems offers an effective way to overcome scintillation. The bit error rate (BER) with respect to different parameters like average SNR, link distance at various weather conditions are also simulated. The simulation results are verified in Matlab environment with the mathematical analysis [4]. The spatial diversity techniques like EGC and MRC in FSO communication systems employing the hybrid PPM-

BPSK-SIM modulation scheme. The study shows that the hybrid PPM-BPSK-SIM modulation has a noticeable improvement is about 6.5 dB compared to BPSK-SIM technique in the BER performance. It is observed from the simulation result that unlike single input single output (SISO) system, an increase in the number receivers for single input multiple output (SIMO) system results in better system performance as N= 1 to N= 4 in clear air condition the BER improvement is about 4.7 dB and in light fog case it is about 13.3 dB in [4]. But in different weather condition, when attenuation level increases from clear air condition to light fog condition, the bit error rate decreases but the application of hybrid PPM BPSK- SIM with higher order diversity improves the BER performance. It is observed from the simulation that changing rate of BER in higher diversity order N= 4 (1 x 4 SIMO) is very less compared to N= 1 (1 x 1 SISO) from clear air condition to light fog condition. Thus hybrid PPM-BPSKSIM modulation scheme with spatial diversity can be a better approach for mitigation of scintillation up to some extent [4].

The BER under DPSK modulation and ergodic capacity of FSO rely system including dual hop RF FSO and FSO-FSO links is evaluated [5]. We study the dual-branch FSO selection combining and dual hop variable gain FSO relay operating on such channels with the impact of pointing errors to show diversity enhancement on the system performance and capacity. First, we express the statistical properties of the maximum and the minimum of double generalized gamma random variables under the impact of pointing errors in terms of H-function and G-function. In particular, we find the cumulative distribution function (CDF), the probability density function (PDF), the moment generating function (MGF), and the moments in closed-form [5].

The BER performance of FSO links with spatial diversity over atmospheric turbulence channels described by the Double GG distribution is analyzed and obtained an efficient and unified closed-form expression for the BER of SIMO FSO systems with OC receiver which generalizes existing results as special cases [6]. For MISO and MIMO systems, BER performance based on numerical calculations of the integral expressions has been presented. The numerical results have demonstrated that spatial diversity schemes can significantly improve the system performance and bring impressive performance gains over SISO systems. The error rate performance of single-input multiple-output (SIMO), multiple-input single-output (MISO) and MIMO FSO systems employing intensity modulation/direct detection (IM/DD) with on-off keying (OOK) over independent and not necessarily identically distributed (i.i.d.) Double GG turbulence channels [6].

7.	Aminikashani, M., Kavehrad, M. and Gu, W., 2016, February. Error performance analysis of FSO links with equal gain diversity receivers over double generalized gamma fading channels. In *Broadband Access Communication Technologies X* (Vol. 9772, p. 97720R). International Society for Optics and Photonics.[7]	BER performance of FSO systems with transmit diversity or receive diversity with equal gain combining (EGC) over atmospheric turbulence channels described by the Double Generalized Gamma (Double GG) distribution.	MIMO system is not considered.
8.	Jagadeesh, V.K., Palliyembil, V., Muthuchidambaranathan, P. and Bui, F.M., 2015. Free space optical communication using subcarrier intensity modulation through generalized turbulence channel with pointing error. *Microwave and Optical Technology Letters*, *57*(8), pp.1958-1961.[8]	The effects of channel turbulence and pointing error are investigated by deriving the closed form expressions for the ABER and ergodic channel capacity for a BPSK-SIM FSO system.	BPSK-SIM is used but MPSK which is a better modulation scheme, is not analyzed. MIMO system is also not considered in this paper.

9.	Bhatnagar, M.R. and Ghassemlooy, Z., 2016. Performance analysis of gamma–gamma fading FSO MIMO links with pointing errors. *Journal of Lightwave technology*, *34*(9), pp.2158-2169.[9]	Average SER is derived for both EGC and MRC. Analytical diversity order and combining gain for both systems are also obtained.	Gamma-Gamma distribution is used which does not work for strong turbulence conditions whereas double generalized gamma distribution is not considered.

A major performance limiting factor in FSO systems is atmospheric turbulence which severely degrades the system performance. To address this issue, multiple transmit and/or receive apertures can be employed, and the performance can be improved via diversity gain. A closed-form union upper bound for the pdf of the sum of Double GG distributed RVs has been derived. A novel union upper bound for the average BER as well as corresponding asymptotic expression is then derived and evaluated in terms of Meijer G-functions [7]. Using this bound, we have investigated the BER performance of FSO links with receive diversity employing equal gain combining over Double GG turbulence channels. An efficient and unified upper bound for the average BER of SIMO FSO systems with EGC receiver has been obtained which generalizes BER results over other atmospheric turbulence models as special cases [7]. Based on the asymptotical performance analysis, we have further derived diversity gains for SIMO FSO systems under consideration.

The performance of subcarrier intensity modulation and effects of channel turbulence and pointing error on system has been analyzed [8]. System suffers degradation due to channel turbulence and pointing error. The pointing error occurs due to the misalignment in the line of sight between transmitter and receiver. Channel model used is Malaga distribution which covers all channel condition from weak to strong turbulence and pointing error. The system model used is BPSK-SIM, subcarrier intensity modulation is used to multiplex different user on to the same channel at the same time by modulating each user information with carrier signals. This signal is then used to modulate the irradiance of the optical generator. The closed form analytical expression for bit error and channel capacity is also derived. The results has shown the performance deterioration the system suffers because of the channel and also how the m-distribution model can be used to obtain the performance over other FSO channels [8].

A general system and realistic study of the FSO multiple-input multiple-output (MIMO) system is done in [9]. The effect of Probability Error in the Gamma-Gamma (GG) fading atmospheric fluctuations is considered in this paper. In this two schemes for the FSO MIMO system are analyzed that are equal gain combining (EGC) and maximal ratio combining (MRC). Power series based representation is proposed for PDF of generalized fading. It contains exponent of random variable as compared to closed -form representation. The SIM scheme with M-ary PSK (MPSK) modulation is adopted for the performance analysis. Average SER is derived for both EGC and MRC. Analytical diversity order and combining gain for both systems are also obtained. Effect of pointing error over performance is analyzed [9]. The proposed analysis give us asymptotic properties of the FSO MIMO system in presence of the PEs. It is observed from [9] that EGC scheme is simpler to implement but MRC scheme is more effective for large Pointing errors. Meijer-G function based PDF expression of GG fading FSO link is difficult to study effect of pointing error in FSO MIMO over SNR range.

10.	Li, J., Liu, J.Q. and Taylor, D.P., 2007. Optical communication using subcarrier PSK intensity modulation through atmospheric turbulence channels.[10]	The BER is derived for optical communication systems employing either on/off key (OOK) or subcarrier PSK intensity modulation.	Log normal distribution is considered therefore strong turbulence condition is not analyzed.
11.	Kaur, P., Jain, V.K. and Kar, S., 2015. Performance analysis of free space optical links using multi-input multi-output and aperture averaging in presence of turbulence and various weather conditions. *IET Communications*, *9*(8), pp.1104-1109.[11]	Performance of FSO link under various weather conditions is evaluated in terms of BER, outage probability and diversity gain.	Gamma-Gamma distribution is used which does not work for strong turbulence conditions.

12.	Saeed, R.A. and Abbas, E.B., 2018, August. Performance Evaluation of MIMO FSO Communication with Gamma-Gamma Turbulence Channel using Diversity Techniques. In *2018 International Conference on Computer, Control, Electrical, and Electronics Engineering (ICCCEEE)* (pp. 1-5). IEEE.[12]	Analyzed BER for different combining techniques and found that system performance increased. Examined the diversity combining techniques to minimize fading.	Double generalized gamma distribution is not employed.

Optical communications using subcarrier phase shift keying (PSK) intensity modulation through atmospheric turbulence channels is studied in [10]. The bit error rate (BER) is derived employing either OOK or subcarrier PSK intensity modulation. It is shown that signal scintillation caused by atmospheric turbulence severely degrades the performance of optical communication systems. When the detector collection aperture reaches some certain size, increasing it will not help further reduce the scintillation level. It was shown that subcarrier phase-shift keying (PSK) intensity modulation was superior to OOK in the presence of atmospheric turbulence. Analysis of BER for optical communication systems using OOK and disadvantage is identified. Analysis of the BER for optical communication systems employing subcarrier PSK intensity modulation [10]. Simulation results are presented for optical communications systems employing convolutional codes with either OOK or subcarrier PSK intensity modulation. Convolutional codes are discussed for optical communication through atmospheric turbulence channels.

The effect of multi-input multi-output (MIMO) spatial diversity schemes when used in a free space optical (FSO) communication link in the presence of turbulence and varied weather conditions such as very clear air, drizzle, haze, fog is studied in [11]. The performance is evaluated in terms of the bit error rate (BER) and outage probability Pout. It shows that MIMO schemes cause a decrease in the BER and Pout which at low signal-to-noise ratios is more significant in presence of very clear air and clear air as compared with haze and fog weather conditions. The performance of FSO link with MIMO schemes is compared with a FSO link using aperture averaging [11]. Owing to constraint on the receiver aperture diameter, the aperture averaging technique fails to give the same kind of performance as provided by the higher order MIMO schemes.

Free Space Optical (FSO) communication has been evaluated in indoor and outdoor experimental environments for other communication applications, which opens the study of environmental effects in FSO communications, these effects represents the nature environments around us such as rain and fog, which are termed by mathematical distribution models such as lognormal and Gamma-gamma distribution. One of the major solutions that proposed to reduce these effects and enhance the received signal is the use of Multiple Input Multiple Output MIMO diversity techniques in FSO. A Multi-input Multi-output free space optical channel model is impaired with atmospheric turbulence, gamma-gamma distribution and the diversity gain only on the atmospheric parameters; also it is independent from the number of transceivers and atmospheric fading parameters [12]. The bit error rate for different diversity combining techniques is analysed and it is found that the system performance is increased. Another different procedure has been utilized to examine the diversity combining techniques to minimize the fading and also as a solution for conflicting turbulence-induced fading over FSO links [12].

13.	Johnsi, A.A. and Saminadan, V., 2013, April. Performance of diversity combining techniques for fso-mimo system. In *2013 International Conference on Communication and Signal Processing* (pp. 479-483). IEEE.[13]	Analyzed BER and outage probability for different combining techniques which increases system performance.	Log normal distribution is considered therefore strong turbulence condition is not analyzed.
14.	Saber, M.J. and Keshavarz, A., 2018, May. On performance of adaptive	Performance evaluation of adaptive subcarrier PSK	PSK is used which has lower bandwidth efficiency.

	subcarrier intensity modulation over generalized FSO links. In *Electrical Engineering (ICEE), Iranian Conference on* (pp. 358-361). IEEE.[14]	intensity modulation for FSO communication system over Malaga turbulence channel.	
15.	Sadiku, M.N., Musa, S.M. and Nelatury, S.R., 2016. Free space optical communications: An overview. *European scientific journal*, *12*(9).[15]	Basic concepts of Free Space Optical communication, its advantages and limitation.	-

Atmospheric turbulence causes random fluctuations in transmitting laser beam which gives rise to scintillation. Compared to the large data rates, scintillation process is slow in optical transmission. In order to mitigate this harmful effect of atmospheric turbulence and beam wander, multiple input and multiple output (MIMO) is used. The mitigation of scintillation is achieved through multiple lasers and multiple output apertures, thereby creating a multiple input multiple output (MIMO) channel. In MIMO system different diversity combining techniques are used. A model for FSO-MIMO channels impaired in the presence of atmospheric fading, the diversity gain depends only on the atmospheric parameters and is independent of both the number of transceivers and atmospheric fading parameters [13]. The bit error rate and the outage probability are analysed for different diversity combining techniques which increases the performance of the system. The results confirm that the performance of the threshold combining is better when compared with the EGC, SC and MRC techniques [13]. By increasing the number of transmitter antennas and receiver antennas, diversity gain is increased and the performance of the system is increased. In order to reduce fading an alternative approach is used to investigate the cooperative diversity technique as a solution for combating turbulence-induced fading over Free-Space Optical (FSO) links.

An adaptive subcarrier phase shift keying (PSK) intensity modulation for free space optical (FSO) communication systems operating over Malaga atmospheric turbulence channel, which is a generalized statistical model proposed for FSO communications is studied in [14]. According to the instantaneous state of turbulence-induced irradiance fluctuation and a target bit error rate (BER), the proposed transmission technique offers efficient utilization of the FSO channel capacity by exploiting adaptively the modulation order of subcarrier PSK. Moreover a closed-form expressions for the average BER of non-adaptive strategy, the achievable spectral efficiency and the average BER of proposed adaptive subcarrier PSK FSO system are derived in terms of the Meijer's *G*-function [14]. Numerical results indicate that by using the proposed scheme, achievable spectral efficiency gain is offered without increasing the transmitted average optical power or sacrificing BER requirements.

Bridging the so-called "last mile" in communication networks has revived keen interest in free-Space Optics (FSO), also known as fibre-free or fibreless optics, which is a technology that transports data via laser technology. It is a line-of-sight technology that currently enables optical transmission up to 2.5 Gbps of data, voice and video through the air at long distances (4km), allowing optical connectivity without deploying fiber-optic cable or securing spectrum licenses. It is moving closer to being a realistic alternative to laying fiber in access networks. An introduction to FSO and the current state of its technology is presented in [15]. The growth of communications networks has accelerated last-mile access needs for high speed links. FSO is a viable choice for connecting the LAN, WAN, and MAN; carrying voice, video and data at the speed of light. However, FSO links in the mid-infrared spectrum seem to be more favourable as lower atmospheric transmission losses increase the reliability of the system, particularly under bad weather conditions with low visibility (Martini et al., 2002). While fiber-optic communication has gained acceptance in the telecommunications industry, FSO communication is still a relatively new entrant [15]. Its apprehension has not been universal; its development activity has been concentrated in the US. Its primary advantages are high throughput, solid security, and low cost. with current availability of up to 1.25 Gbps, throughputs of hundreds of Gbps are possible in the future. Free space optics is a technology that is poised for exponential growth in the coming years [15].

16.	Vellakudiyan, J., Muthuchidambaranathan, P., Bui, F.M. and Palliyembil, V., 2015.	Performance analysis of DPSK SIM based FSO system. Expression for BER,	DPSK is used which is highly sensitive to phase noise effects.

	Performance of a subcarrier intensity modulated differential phase-shift keying over generalized turbulence channel. *AEU-International Journal of Electronics and Communications*, *69*(11), pp.1569-1573.[16]	channel capacity and outage probability of the system.	
17.	Dabiri, M.T., Sadough, S.M.S. and Khalighi, M.A., 2017. FSO channel estimation for OOK modulation with APD receiver over atmospheric turbulence and pointing errors. *Optics Communications*, *402*, pp.577-584.[17]	BER performance of EM channel estimator is analyzed.	OOK modulation is used, which offers lower power efficiency and is very susceptible to noise interference.
18.	Kaur, G., Singh, H. and Sappal, A.S., 2017. Free space optical using different modulation techniques—a review. *International Journal of Engineering Trends and Technology (IJETT)*, *43*(2).[18]	Methods for performance enhancement of FSO link are described in this paper.	DPIM and DPPM can also be employed.

The performance of a subcarrier intensity modulated differential phase-shift keying for FSO communication system was presented by considering atmospheric turbulence [16]. A new generic model called M-distribution is used to model the fading channel, this can express all the previous conventional channel model just by varying various parameters. An exact closed form analytical expression for average BER, channel capacity and outage probability was derived for the proposed system which can be applied for the analysis of the conventional previously proposed channel model like gamma–gamma and K-distribution channel models [16].

The case of long-range FSO links with APD-based receivers is considered and optimal signal demodulation for the case of NRZ OOK signaling is investigated, in the presence of signal-dependent shot noise [17]. Due to the computational complexity of the estimators, we then proposed an ML channel estimator based on the iterative EM algorithm. In [17] we investigated the performance of the proposed EM-based estimator through numerical simulations, which alleviated the advantage of this estimator compared to the three other methods. The relatively low computational complexity and the low estimation delay of the proposed method and the fact that it does not rely on the transmission of pilot sequences, makes it particularly suitable for implementation in FSO communication links.

Free space optics is replacing radio frequency communication because of its high speed, large bandwidth, maximum performance, minimum error and efficient communication. All these can be achieved by using free space optical communication system. Because FSO system is license free and cost effective, therefore, it has become need of the hour. Turbulence manifests in increased Bit Error Rate (BER) leading to degradation in the link performance. In [18] a comprehensive survey of FSO communication system with main focus on the study of different turbulent conditions of atmosphere is done. Moreover, work done by different researchers in the field of FSO system using different modulation techniques in various turbulence models is discussed. Also, methods for performance enhancement of FSO link are described in the work.

19.	Popoola, W.O. and Ghassemlooy, Z., 2009. BPSK subcarrier intensity modulated free-space optical communications in atmospheric turbulence. *Journal of Lightwave*	The BER expression for SIM terrestrial FSO link has been presented in all turbulence regimes from weak to saturation.	Spatial diversity is used which is only used for strong turbulence.

	technology, *27*(8), pp.967-973.[19]		
20.	Prabu, K. and Kumar, D.S., 2015. BER analysis for BPSK based SIM–FSO communication system over strong atmospheric turbulence with spatial diversity and pointing errors. *Wireless Personal Communications*, *81*(3), pp.1143-1157.[20]	The exact closed-form expressions for the average BER of BPSK-SIM based SISO and SIMO–FSO systems over a strong atmospheric channel with pointing errors are derived.	MIMO system is not employed. Spatial diversity is used which is only used for strong turbulence.

Free-space optical communications (FSO) propagated over a clear atmosphere suffers from irradiance fluctuation caused by small but random atmospheric temperature fluctuations. This results in decreased signal-to-noise ratio (SNR) and consequently impaired performance. The error performance of the FSO using a subcarrier intensity modulation (SIM) based on a binary phase shift keying (BPSK) scheme in a clear but turbulent atmosphere is presented [19]. To evaluate the system error performance in turbulence regimes from weak to strong, the probability density function (pdf) of the received irradiance after traversing the atmosphere is modelled using the gamma-gamma distribution while the negative exponential distribution is used to model turbulence in the saturation region and beyond. The effect of turbulence induced irradiance fluctuation is mitigated using spatial diversity at the receiver [19].

The error rate performance of binary phase shift keying-based subcarrier intensity modulated free space optical (SIM–FSO) communication system over gamma–gamma channel with pointing errors is investigated [20]. Novel closed-form analytical expressions are derived for the average bit error rate of single-input multiple-output FSO (SIMO–FSO) system with various combining schemes. In [20] it is observed that SC provides the best BER performance compared to other considered combining schemes. It is also shown that a large number of receiving apertures offer a better BER performance. In addition, this work presents the simulation of BER performances of SIMO with a maximum of seven receiver apertures. A better BER performance is achieved by using SIMO with SC combining is 10−5 at SNR = 30 dB.

CHAPTER 3

MATHEMATICAL MODEL

3.1 INTRODUCTION

A major performance limiting factor in FSO systems is atmospheric turbulence-induced fading (also called as scintillation). Inhomogeneities in the temperature and the pressure

of the atmosphere result in variations of the refractive index and cause atmospheric turbulence. This manifest itself as random fluctuations in the received signal and severely degrades the FSO system performance particularly over long ranges.

Various statistical models have been proposed in several literatures in an effort to model this random phenomenon. Some pdf models are only applicable to weak turbulence

conditions and some in only strong turbulence conditions.

Out of these pdf models Double Generalized Gamma (Double GG) model is valid under all range of turbulence conditions (weak to strong).

We have reproduced the PDF of double generalized gamma distribution in term of Fox's h function as it difficult to deal with the fox's h function so we expand it into infinite series for the simplicity of calculation.

3.1.1 PDF OF DOUBLE GENERALIZED GAMMA DISTRIBUTION

The double Generalized distribution is obtained from Generalized Gamma Distribution of small scale and large-scale irradiance fluctuation $I_x \ and \ I_y$ modelled as $I = I_x I_y$ and their PDFs are as follows,

$$f_{I_x}(Ix) = \frac{\gamma_1 I_x^{m_1\gamma_1 - 1}}{(\Omega 1/m1)^{m_1}\Gamma(m1)} exp\left(-\frac{m1}{\Omega 1} I_x^{\gamma 1}\right) \tag{3.1}$$

$$f_{I_y}(Iy) = \frac{\gamma_2 I_y^{m_2\gamma_2 - 1}}{(\Omega 2/m2)^{m2}\Gamma(m2)} exp\left(-\frac{m2}{\Omega 2} I_y^{\gamma_2}\right) \tag{3.2}$$

where $\gamma_i > 0$, $m_i > 0.5$ and Ω_i, i = 1, 2 are the parameters of the generalized gamma distribution. I is the irradiance of the received optical wave. Thus, the PDF of I can be derived by

$$f_I(I) = \int_0^\infty f_{I_x}(I/I_y) f_{I_y}(Iy)\, dI_y \tag{3.3}$$

where $f_{I_x}(I/I_y)$ is obtained as,

$$f_{I_x}\left(I/I_y\right) = \frac{\gamma_1 (I/I_y)^{m1\gamma1-1}}{Iy(\Omega_1/m_1)^{m1}\Gamma(m1)} \, exp\left(-\frac{m1}{\Omega1}\left(\frac{I}{I_y}\right)^{\gamma1}\right) \tag{3.4}$$

with the help of [21, Eq (5.5)], the integration in (2.3) yields

$$f_I = \frac{\gamma}{I\,\Gamma(m_1)\Gamma(m_2)} \quad H_{2,0}^{0,2}\left[\frac{\Omega_1}{I^{\gamma_1} m_1}\left(\frac{\Omega_2}{m_2}\right)^{\frac{\gamma_1}{\gamma_2}}\middle|(1-m_1,1)\left(1-m_2,\frac{\gamma_1}{\gamma_2}\right)\right] \tag{3.5}$$

where $H_{2,0}^{0,2}(\,)$ is the Fox's H-function.

To avoid dealing with the Fox's H-function, we have expanded it into an infinite power series by using [22, Th.1.4], and therefore obtain the series representation form of the double GG PDF:

$$f_I(I) = \sum_{l=0}^{\infty}(a_l(m_1\gamma_1, m_2\gamma_2) I^{l\gamma_1+m_1\gamma_1-1} + \; a_l(m_1\gamma_1, m_2\gamma_2) I^{l\gamma_1+m_1\gamma_1-1}) \tag{3.6}$$

where

$$a_l(m_1\gamma_1, m_2\gamma_2) = \frac{\gamma_1}{\Gamma(m1)\Gamma(m2)} \, \frac{(-1)^l}{l!} \; \Gamma\left(m_2 - (m_1+l)\frac{\gamma_1}{\gamma_2}\right)\left(\frac{m_1}{\Omega_1}\left(\frac{m_2}{\Omega_2}\right)^{\frac{\gamma_1}{\gamma_2}}\right)^{(l+m_1)} \tag{3.7}$$

$$a_l(m_2\gamma_2, m_1\gamma_1) = \frac{\gamma_2}{\Gamma(m1)\Gamma(m2)} \frac{(-1)^l}{l!} \Gamma\left(m_1 - (m_2+l)\frac{\gamma_2}{\gamma_1}\right)\left(\frac{m_2}{\Omega_2}\left(\frac{m_1}{\Omega_1}\right)^{\frac{\gamma_2}{\gamma_1}}\right)^{(l+m_2)} \tag{3.8}$$

3.1.2 POST DETECTION ELECTRICAL SNR FOR RC MIMO

For RC MIMO FSO system involving n_T lasers and n_R photodetectors, the expression for post detection SNR is:

$$\gamma_{RC} = \frac{\bar{\gamma}}{{n_T}^2 n_R}\left[\sum_{i=1}^{n_R}\sum_{j=1}^{n_T} I_{ij}\right]^2 \tag{3.9}$$

Where, $\bar{\gamma}$ is the average electrical SNR and I_{ij} is the instantaneous channel fading coefficient between j^{th} lasers and i^{th} photodetector.

It is assumed that the I_{ij}'s are independent and identically distributed (i.i.d.) random variates (RVs) with their PDFs following the same double GG distribution.

3.1.3 AVERAGE SYMBOL ERROR RATE OF SUBCARRIER MPSK FOR MIMO FSO SYSTEM WITH RC SCHEME

From equation (.6) and the assumption that I_{ij} has PDF following the same double GG distribution.

$$f_{I_{ij}}(I_{ij}) = \sum_{l=0}^{\infty}(a_l(m_1\gamma_1, m_2\gamma_2){I_{ij}}^{l\gamma_1+m_1\gamma_1-1} + a_l(m_1\gamma_1, m_2\gamma_2){I_{ij}}^{l\gamma_1+m_1\gamma_1-1}) \tag{3.10}$$

where

$$a_l(m_1\gamma_1, m_2\gamma_2) = \frac{\gamma_1}{\Gamma(m1)\Gamma(m2)}\ \frac{(-1)^l}{l!}\ \Gamma\left(m_2 - (m_1 + l)\frac{\gamma_1}{\gamma_2}\right)(\frac{m_1}{\Omega_1}(\frac{m_2}{\Omega_2})^{\frac{\gamma_1}{\gamma_2}})^{(l+m_1)} \tag{3.11}$$

$$a_l(m_2\gamma_2, m_1\gamma_1) = \frac{\gamma_2}{\Gamma(m1)\Gamma(m2)}\frac{(-1)^l}{l!}\Gamma\left(m_1 - (m_2 + l)\frac{\gamma_2}{\gamma_1}\right)(\frac{m_2}{\Omega_2}(\frac{m_1}{\Omega_1})^{\frac{\gamma_2}{\gamma_1}}))^{(l+m_2)} \tag{3.12}$$

The Moment Generating Function (MGF) of I_{ij} can be derived in terms of power series:

$$M_{I_{ij}}(s) = \int_0^{\infty} e^{-s\,I_{ij}} f_{I_{ij}}(\,I_{ij})\,dI_{ij} \tag{3.13}$$

Using equation (3.10) and (3.13)

$$M_{I_{ij}}(s) = \int_0^{\infty} e^{-sI_{ij}} \sum_{l=0}^{\infty}\left[a_l(m_1\gamma_1, m_2\gamma_2){I_{ij}}^{l\gamma_1+m_1\gamma_1-1} + a_l(m_2\gamma_2, m_1\gamma_1){I_{ij}}^{l\gamma_1+m_2\gamma_2-1}\right]dI_{ij} \tag{3.14}$$

$$M_{I_{ij}}(s) = \int_0^{\infty} e^{-sI_{ij}} \sum_{l=0}^{\infty} a_l(m_1\gamma_1, m_2\gamma_2){I_{ij}}^{l\gamma_1+m_1\gamma_1-1}dI_{ij} + \int_0^{\infty} e^{-sI_{ij}} \sum_{l=0}^{\infty} a_l(m_2\gamma_2, m_1\gamma_1){I_{ij}}^{l\gamma_1+m_2\gamma_2-1}dI_{ij} \tag{3.15}$$

Considering the first integral of equation (3.15),

$$\sum_{l=0}^{\infty} a_l(m_1\gamma_1, m_2\gamma_2)\int_0^{\infty} e^{-sI}{I_{ij}}^{l\gamma_1+m_1\gamma_1-1}\,dI_{ij} \tag{3.16}$$

From equation 3.478(1), Ref 23 we get,

$$\int_0^{\infty} x^{v-1}exp(-\mu x^p)dx = \frac{1}{p}\mu^{-\frac{v}{p}}\Gamma\left(\frac{v}{p}\right) \tag{3.17}$$

Comparing equations (3.16) and (3.17), we get

$$\mu = s,\ x = I_{ij},\ p = 1,\ v = l\gamma_1 + m_1\gamma_1 \tag{3.18}$$

Now, equations (3.16) becomes:

$$\sum_{l=0}^{\infty} a_l(m_1\gamma_1, m_2\gamma_2)s^{-(l\gamma_1+m_1\gamma_1)}\Gamma(l\gamma_1 + m_1\gamma_1) \tag{3.19}$$

Similarly, the second integral of equation (3.15) becomes:

$$\sum_{l=0}^{\infty} a_l(m_2\gamma_2, m_1\gamma_1)s^{-(l\gamma_2+m_2\gamma_2)}\Gamma(l\gamma_2 + m_2\gamma_2) \tag{3.20}$$

Now equation (3.15) can be rewritten as:

$$\begin{aligned} M_{I_{ij}}(s) = &\sum_{l=0}^{\infty}\left[a_l(m_1\gamma_1, m_2\gamma_2)s^{-(l\gamma_1+m_1\gamma_1)}\Gamma(l\gamma_1 + m_1\gamma_1)\right] \\ &+\sum_{l=0}^{\infty}\left[a_l(m_2\gamma_2, m_1\gamma_1)s^{-(l\gamma_2+m_2\gamma_2)}\Gamma(l\gamma_2 + m_2\gamma_2)\right] \end{aligned} \tag{3.21}$$

Or

$$M_{I_{ij}}(s) = \sum_{l=0}^{\infty} \tilde{b}_l(m_1\gamma_1, m_2\gamma_2)s^{-m_1\gamma_1-l\gamma_1} + \sum_{l=0}^{\infty} \tilde{b}_l(m_2\gamma_2, m_1\gamma_1)s^{-m_2\gamma_2-l\gamma_2} \tag{3.22}$$

Where

$$\tilde{b}_l(m_1\gamma_1, m_2\gamma_2) = a_l(m_1\gamma_1, m_2\gamma_2)\Gamma(l\gamma_1 + m_1\gamma_1) \tag{3.23}$$

$$\tilde{b}_l(m_2\gamma_2, m_1\gamma_1) = a_l(m_2\gamma_2, m_1\gamma_1)\Gamma(l\gamma_2 + m_2\gamma_2) \tag{3.24}$$

Now, let

$$Y = \sum_{i=1}^{n_R}\sum_{j=1}^{n_T} I_{ij} \tag{3.25}$$

Since I_{ij}'s are assumed to be i.i.d. RVs, MFG of Y can be expressed as:

$$M_Y(s) = \left(M_{ij}(s)\right)^{n_T n_R} \tag{3.26}$$

From equations (3.22) and (3.26),

$$\begin{aligned} M_Y(s) = &\left[\sum_{l=0}^{\infty} \tilde{b}_l(m_1\gamma_1, m_2\gamma_2)s^{-m_1\gamma_1-l\gamma_1}\right. \\ &\left.+\sum_{l=0}^{\infty} \tilde{b}_l(m_2\gamma_2, m_1\gamma_1)s^{-m_2\gamma_2-l\gamma_2}\right]^{n_T n_R} \end{aligned} \tag{3.27}$$

By using Binomial Theorem, we get

$$M_Y(s) = \sum_{k=0}^{n_T n_R} \binom{n_T n_R}{k} \left[\sum_{l=0}^{\infty} \tilde{b}_l(m_1\gamma_1, m_2\gamma_2) s^{-m_1\gamma_1 - l\gamma_1}\right]^{n_T n_R - k}$$
$$\left[\sum_{l=0}^{\infty} \tilde{b}_l(m_2\gamma_2, m_1\gamma_1) s^{-m_2\gamma_2 - l\gamma_2}\right]^{k} \tag{3.28}$$

$$M_Y(s) = \sum_{k=0}^{n_T n_R} \binom{n_T n_R}{k} \left[\sum_{l=0}^{\infty} \tilde{b}_l(m_1\gamma_1, m_2\gamma_2)\right]^{n_T n_R - k}$$
$$\left[\sum_{l=0}^{\infty} \tilde{b}_l(m_2\gamma_2, m_1\gamma_1)\right]^{k} s^{-m_1\gamma_1(n_T n_R - k) - k m_2\gamma_2} \tag{3.29}$$

By using equation 0.314, Ref. 23 we get,

$$\left[\sum_{k=0}^{\infty} a_k x^k\right]^n = \sum_{k=0}^{\infty} c_k x^k \tag{3.30}$$

Where

$$c_0 = a_0^n,\ c_m = \frac{1}{m a_0} \textstyle\sum_{k=1}^{m} (kn - m + k) a_k c_{m-k} \tag{3.31}$$

for $m \geq 1,$ and n is a natural number

Using equation (3.29) and (3.30), we get

$$M_Y(s) = \sum_{k=0}^{n_T n_R} \binom{n_T n_R}{k} \left[\sum_{l=0}^{\infty} \tilde{c}_l(m_1\gamma_1, m_2\gamma_2) s^{-l\gamma_1}\right] \left[\sum_{l=0}^{\infty} \tilde{c}_l(m_2\gamma_2, m_1\gamma_1) s^{-l\gamma_2}\right]$$
$$s^{-m_1\gamma_1(n_T n_R - k) - k m_2\gamma_2} \tag{3.32}$$

Where

$$\tilde{c}_0(m_1\gamma_1, m_2\gamma_2) = \left[\tilde{b}_0(m_1\gamma_1, m_2\gamma_2)\right]^{n_T n_R - k} \tag{3.33}$$

$$\tilde{c}_0(m_2\gamma_2, m_1\gamma_1) = \left[\tilde{b}_0(m_2\gamma_2, m_1\gamma_1)\right]^{k} \tag{3.34}$$

$$\tilde{c}_m(m_1\gamma_1, m_2\gamma_2) = \frac{1}{m\tilde{b}_0(m_1\gamma_1, m_2\gamma_2)} \sum_{l=1}^{m} (l(n_T n_R - k) - m + l)$$
$$\tilde{b}_0(m_1\gamma_1, m_2\gamma_2) \tilde{c}_{m-l}(m_1\gamma_1, m_2\gamma_2) \tag{3.35}$$

$$\tilde{c}_m(m_2\gamma_2, m_1\gamma_1) = \frac{1}{m\tilde{b}_0(m_2\gamma_2, m_1\gamma_1)} \sum_{l=1}^{m} (lk - m + l)\, \tilde{b}_0(m_2\gamma_2, m_1\gamma_1)$$
$$\tilde{c}_{m-l}(m_2\gamma_2, m_1\gamma_1) \tag{3.36}$$

From the principle of multiplication of infinite series,

$$\left(\sum_{i=0}^{\infty} a_i\right)\left(\sum_{j=0}^{\infty} b_j\right) = \sum_{i=0}^{\infty}\sum_{j=0}^{i} a_j b_{i-j} \tag{3.37}$$

Equation (3.32) can be rewritten as

$$M_Y(s) = \sum_{k=0}^{n_T n_R} \binom{n_T n_R}{k} \sum_{i=0}^{\infty}\sum_{j=0}^{i} \tilde{c}_j(m_1\gamma_1, m_2\gamma_2)\tilde{c}_{i-j}(m_2\gamma_2, m_1\gamma_1)$$
$$s^{-m_1\gamma_1(n_T n_R - k) - k m_2\gamma_2 - j\gamma_1 - (i-j)\gamma_2} \tag{3.38}$$

From the definition of Inverse Laplace

$$f_Y(y) = \frac{1}{2\pi i}\oint M_Y(s) e^{ys} ds \tag{3.39}$$

From equation (8.315) Ref. 23, we get

$$\frac{1}{\Gamma z} = \frac{i}{2\pi}\oint (-t)^{-z} e^{-t} dt\,, \quad OR \quad \oint (-t)^{-z} e^{-t} dt = \frac{2\pi}{i\Gamma z} \tag{3.40}$$

From equations (3.38) and (3.39)

$$f_Y(y) = \frac{1}{2\pi i}\oint \sum_{k=0}^{n_T n_R} \binom{n_T n_R}{k} \sum_{i=0}^{\infty}\sum_{j=0}^{i} \tilde{c}_j(m_1\gamma_1, m_2\gamma_2)\tilde{c}_{i-j}(m_2\gamma_2, m_1\gamma_1)$$
$$s^{-m_1\gamma_1(n_T n_R - k) - k m_2\gamma_2 - j\gamma_1 - (i-j)\gamma_2} e^{ys} ds \tag{3.41}$$

$$f_Y(y) = \frac{1}{2\pi i}\sum_{k=0}^{n_T n_R} \binom{n_T n_R}{k} \sum_{i=0}^{\infty}\sum_{j=0}^{i} \tilde{c}_j(m_1\gamma_1, m_2\gamma_2)\tilde{c}_{i-j}(m_2\gamma_2, m_1\gamma_1)$$
$$\oint s^{-(n_T n_R - k) m_1\gamma_1 - k m_2\gamma_2 - j\gamma_1 - (i-j)\gamma_2} e^{ys} ds \tag{3.42}$$

Substituting, $s = -\frac{t}{y}$ $and\ ds = -\frac{dt}{y}$ in equation (2.42), we get

$$f_Y(y) = -\frac{1}{2\pi y i}\sum_{k=0}^{n_T n_R} \binom{n_T n_R}{k} \sum_{i=0}^{\infty}\sum_{j=0}^{i} \tilde{c}_j(m_1\gamma_1, m_2\gamma_2)\tilde{c}_{i-j}(m_2\gamma_2, m_1\gamma_1)$$
$$\oint \left(-\frac{t}{y}\right)^{-(n_T n_R - k) m_1\gamma_1 - k m_2\gamma_2 - j\gamma_1 - (i-j)\gamma_2} e^{-t} dt \tag{3.43}$$

$$f_Y(y) = -\frac{1}{2\pi i}\sum_{k=0}^{n_T n_R} \binom{n_T n_R}{k} \sum_{i=0}^{\infty}\sum_{j=0}^{i} \tilde{c}_j(m_1\gamma_1, m_2\gamma_2)\tilde{c}_{i-j}(m_2\gamma_2, m_1\gamma_1) \tag{3.44}$$

$$y^{(n_T n_R - k)m_1\gamma_1 + km_2\gamma_2 + j\gamma_1 + (i-j)\gamma_2 - 1} \oint (-t)^{-(n_T n_R - k)m_1\gamma_1 - km_2\gamma_2 - j\gamma_1 - (i-j)\gamma_2} e^{-t} dt$$

By using equation (3.40), equation (3.44) can be rewritten as:

$$f_Y(y) = -\frac{1}{2\pi i} \sum_{k=0}^{n_T n_R} \binom{n_T n_R}{k} \sum_{i=0}^{\infty} \sum_{j=0}^{i} \tilde{c}_j(m_1\gamma_1, m_2\gamma_2) \tilde{c}_{i-j}(m_2\gamma_2, m_1\gamma_1)$$
$$y^{(n_T n_R - k)m_1\gamma_1 + km_2\gamma_2 + j\gamma_1 + (i-j)\gamma_2 - 1} \frac{2\pi}{i\Gamma\left((n_T n_R - k)m_1\gamma_1 + km_2\gamma_2\right.} \tag{3.45}$$

$$f_Y(y) = \sum_{k=0}^{n_T n_R} \binom{n_T n_R}{k} \sum_{i=0}^{\infty} \sum_{j=0}^{i} \frac{\tilde{c}_j(m_1\gamma_1, m_2\gamma_2) \tilde{c}_{i-j}(m_2\gamma_2, m_1\gamma_1)}{\Gamma\left((n_T n_R - k)m_1\gamma_1 + km_2\gamma_2 + j\gamma_1 + (i-j)\gamma_2\right)}$$
$$y^{(n_T n_R - k)m_1\gamma_1 + km_2\gamma_2 + j\gamma_1 + (i-j)\gamma_2 - 1} \tag{3.46}$$

$$f_X(x) = \sum_{k=0}^{n_T n_R} \binom{n_T n_R}{k} \sum_{i=0}^{\infty} \sum_{j=0}^{i} \frac{\tilde{c}_j(m_1\gamma_1, m_2\gamma_2) \tilde{c}_{i-j}(m_2\gamma_2, m_1\gamma_1)}{\Gamma\left((n_T n_R - k)m_1\gamma_1 + km_2\gamma_2 + j\gamma_1 + (i-j)\gamma_2\right)}$$
$$x^{(n_T n_R - k)m_1\gamma_1 + km_2\gamma_2 + j\gamma_1 + (i-j)\gamma_2 - 1} \tag{3.47}$$

Let $X = Y^2$ represent a RV which depend on the channel fading whose pdf is $f_X(x)$ and is given as,

$$Y = \sqrt{X} \tag{3.48}$$

$$f_X(x) = |J| f_Y(y) \tag{3.49}$$

$$|J| = \frac{\partial x}{\partial y} \tag{3.50}$$

$$\frac{\partial x}{\partial y} = \frac{1}{2\sqrt{y}} \tag{3.51}$$

Substituting the values from equation (3.47) to equation (3.49) we get,

$$f_{Y^2}(y) = \frac{1}{2\sqrt{y}} \sum_{k=0}^{n_T n_R} \binom{n_T n_R}{k} \sum_{i=0}^{\infty} \sum_{j=0}^{i} \frac{\tilde{c}_j(m_1\gamma_1, m_2\gamma_2) \tilde{c}_{i-j}(m_2\gamma_2, m_1\gamma_1)}{\Gamma\left((n_T n_R - k)m_1\gamma_1 + km_2\gamma_2 + j\gamma_1 + (i-j)\gamma_2\right)}$$
$$y^{\frac{(n_T n_R - k)m_1\gamma_1 + km_2\gamma_2 + j\gamma_1 + (i-j)\gamma_2 - 1}{2}} \tag{3.52}$$

$$f_{Y^2}(y) = \frac{1}{2\sqrt{y}} \sum_{k=0}^{n_T n_R} \binom{n_T n_R}{k} \sum_{i=0}^{\infty} \sum_{j=0}^{i} \frac{\tilde{c}_j(m_1\gamma_1, m_2\gamma_2)\tilde{c}_{i-j}(m_2\gamma_2, m_1\gamma_1)}{\Gamma\big((n_T n_R - k)m_1\gamma_1 + km_2\gamma_2 + j\gamma_1 + (i-j)\gamma_2\big)} y^{\frac{(n_T n_R - k)m_1\gamma_1 + km_2\gamma_2 + j\gamma_1 + (i-j)\gamma_2}{2} - 1}\sqrt{y} \quad (3.53)$$

$$f_{Y^2}(y) = \sum_{k=0}^{n_T n_R} \binom{n_T n_R}{k} \sum_{i=0}^{\infty} \sum_{j=0}^{i} \frac{\tilde{c}_j(m_1\gamma_1, m_2\gamma_2)\tilde{c}_{i-j}(m_2\gamma_2, m_1\gamma_1)}{2\Gamma\big((n_T n_R - k)m_1\gamma_1 + km_2\gamma_2 + j\gamma_1 + (i-j)\gamma_2\big)} y^{\frac{(n_T n_R - k)m_1\gamma_1 + km_2\gamma_2 + j\gamma_1 + (i-j)\gamma_2}{2} - 1} \quad (3.54)$$

Now, MFG of Y^2 is given as,

$$M_{Y^2}(s) = \int_0^\infty e^{-sy} f_{Y^2}(y)dy \quad (3.55)$$

$$M_{Y^2}(s) = \int_0^\infty \sum_{k=0}^{n_T n_R} \binom{n_T n_R}{k} \sum_{i=0}^{\infty} \sum_{j=0}^{i} \frac{\tilde{c}_j(m_1\gamma_1, m_2\gamma_2)\tilde{c}_{i-j}(m_2\gamma_2, m_1\gamma_1)}{2\Gamma\big((n_T n_R - k)m_1\gamma_1 + km_2\gamma_2 + j\gamma_1 + (i-j)\gamma_2\big)} y^{\frac{(n_T n_R - k)m_1\gamma_1 + km_2\gamma_2 + j\gamma_1 + (i-j)\gamma_2}{2} - 1} \quad (3.56)$$

Using equation (3.478(1)), Ref. 23 we get,

$$\int_0^\infty x^{v-1} exp(-\mu x^p)dx = \frac{1}{p}\mu^{-\frac{v}{p}}\Gamma\left(\frac{v}{p}\right) \quad (3.57)$$

Comparing equations (3.56) and (3.57) we get,

$$\mu = s,\ x = y,\ p = 1,\ v = \frac{(n_T n_R - k)m_1\gamma_1 + km_2\gamma_2 + j\gamma_1 + (i-j)\gamma_2}{2} \quad (3.58)$$

We get,

$$\int_0^\infty e^{-sy} y^{\frac{(n_T n_R - k)m_1\gamma_1 + km_2\gamma_2 + j\gamma_1 + (i-j)\gamma_2}{2} - 1} dy = \Gamma\left(\frac{(n_T n_R - k)m_1\gamma_1 + km_2\gamma_2 + j\gamma_1 + (i-j)\gamma_2}{2}\right) s^{-\frac{(n_T n_R - k)m_1\gamma_1 + km_2\gamma_2 + j\gamma_1 + (i-j)\gamma_2}{2}} \quad (3.59)$$

Therefore equation (2.56) becomes,

$$M_{Y^2}(s) = \sum_{k=0}^{n_T n_R} \binom{n_T n_R}{k} \sum_{i=0}^{\infty} \sum_{j=0}^{i} \frac{\tilde{c}_j(m_1\gamma_1, m_2\gamma_2)\tilde{c}_{i-j}(m_2\gamma_2, m_1\gamma_1)}{2\Gamma\big((n_T n_R - k)m_1\gamma_1 + km_2\gamma_2 + j\gamma_1 + (i-j)\gamma_2\big)} \quad (3.60)$$

$$\Gamma\left(\frac{(n_T n_R - k)m_1\gamma_1 + km_2\gamma_2 + j\gamma_1 + (i-j)\gamma_2}{2}\right) s^{-\frac{(n_T n_R - k)m_1\gamma_1 + km_2\gamma_2 + j\gamma_1 + (i-j)\gamma_2}{2}}$$

Post detection electrical SNR for RC MIMO system (from equation (3.9)) is,

$$\gamma = \frac{\bar{\gamma}}{n_T^2 n_R}\left(\sum_{i=1}^{n_T}\sum_{j=1}^{n_R} I_{ij}\right)^2 \quad (3.61)$$

The average SER of subcarrier MPSK (from equation (19), Ref 1) is given as,

$$P_e = \frac{1}{\pi}\int_0^{\frac{(M-1)\pi}{M}} M_V\left(\frac{sin^2\left(\frac{\pi}{M}\right)\bar{\gamma}}{sin^2\theta}\right) d\theta \quad (3.62)$$

$$P_e = \frac{1}{\pi}\int_0^{\frac{(M-1)\pi}{M}} M_V\left(\frac{\Bbbk\bar{\gamma}}{sin^2\theta}\right) d\theta \quad (3.63)$$

Where,

$$\Bbbk = sin^2\left(\frac{\pi}{M}\right) \quad (3.64)$$

Electrical SNR for RC MIMO system is,

$$\bar{\gamma} = \frac{\bar{\gamma}}{n_T^2 n_R} \quad (3.65)$$

Now, equation (3.63) becomes,

$$P_{M,\ RC} = \frac{1}{\pi}\int_0^{\frac{(M-1)\pi}{M}} M_{\gamma^2}\left(\frac{\Bbbk\bar{\gamma}}{n_T^2 n_R sin^2\theta}\right) d\theta \quad (3.66)$$

Substituting equations (3.60), (3.64), (3.65) in equation (3.63) we get,

$$P_{M,\ RC} = \frac{1}{\pi}\int_0^{\frac{(M-1)\pi}{M}} \sum_{k=0}^{n_T n_R}\binom{n_T n_R}{k}\sum_{i=0}^{\infty}\sum_{j=0}^{i}\frac{\tilde{c}_j(m_1\gamma_1, m_2\gamma_2)\tilde{c}_{i-j}(m_2\gamma_2, m_1\gamma_1)}{2\Gamma\big((n_T n_R - k)m_1\gamma_1 + km_2\gamma_2 + j\gamma_1 + (i-j)\gamma_2\big)} \quad (3.67)$$

$$\Gamma\left(\frac{(n_T n_R - k)m_1\gamma_1 + km_2\gamma_2 + j\gamma_1 + (i-j)\gamma_2}{2}\right)\left(\frac{\Bbbk\bar{\gamma}}{n_T^2 n_R sin^2\theta}\right)^{-\frac{(n_T n_R - k)m_1\gamma_1 + km_2\gamma_2 + j\gamma_1 + (i-j)\gamma_2}{2}} d\theta$$

Or,

$$P_{M,\ RC} = \sum_{k=0}^{n_T n_R} \binom{n_T n_R}{k} \sum_{i=0}^{\infty} \sum_{j=0}^{i} \frac{\tilde{c}_j(m_1\gamma_1, m_2\gamma_2)\tilde{c}_{i-j}(m_2\gamma_2, m_1\gamma_1)}{2\Gamma\big((n_T n_R - k)m_1\gamma_1 + km_2\gamma_2 + j\gamma_1 + (i-j)\gamma_2\big)} \Lambda_{ij}(n_T n_R, M)\Gamma\left(\frac{(n_T n_R - k)m_1\gamma_1 + km_2\gamma_2 + j\gamma_1 + (i-j)\gamma_2}{2}\right) \left(\frac{\mathcal{k}\bar{\gamma}}{n_T^2 n_R sin^2\theta}\right)^{-\frac{(n_T n_R - k)m_1\gamma_1 + km_2\gamma_2 + j\gamma_1 + (i-j)\gamma_2}{2}} \tag{3.68}$$

Where,

$$\Lambda_{ij}(n_T n_R, M) = \frac{1}{\pi}\int_0^{\frac{(M-1)\pi}{M}} \sin\theta^{(n_T n_R - k)m_1\gamma_1 + km_2\gamma_2 + j\gamma_1 + (i-j)\gamma_2}\, d\theta \tag{3.69}$$

On solving equation (3.69) in Mathematica we get,

$$\Lambda_{ij}(n_T n_R, M) = \frac{\sqrt{\pi}\Gamma\left(\frac{1 + (n_T n_R - k)m_1\gamma_1 + j\gamma_1 + km_2\gamma_2 + (i-j)\gamma_2}{2}\right)}{2\Gamma\left(1 + \frac{(n_T n_R - k)m_1\gamma_1 + j\gamma_1 + km_2\gamma_2 + (i-j)\gamma_2}{2}\right)} - \cos\left(\frac{M-1}{M}\pi\right) 2F1\left[\frac{1}{2}, \frac{1 - (n_T n_R - k)m_1\gamma_1 - j\gamma_1 - km_2\gamma_2 - (i-j)\gamma_2}{2}; \frac{3}{2}; cos^2\left(\frac{M-1}{M}\pi\right)\right] \tag{3.70}$$

Where,

2F1 is a Hypergeometric function.

3.1.4 AVERAGE SYMBOL ERROR RATE OF M-PAM FOR MIMO FSO SYSTEM WITH RC SCHEME

The average SER for M-PAM can be evaluated as

$$P_{M-PAM} = \frac{2}{\pi}\left(1 - \frac{1}{M}\right)\int_0^{\frac{\pi}{2}} M_{Y^2}\left(\frac{\phi\bar{\gamma}}{n_T^2 n_R sin^2\theta}\right) d\theta \tag{3.71}$$

Where,

$$\phi = \frac{3}{(M^2 - 1)} \tag{3.72}$$

And from equation (3.60), we have

$$M_{Y^2}(s) = \sum_{k=0}^{n_T n_R} \binom{n_T n_R}{k} \sum_{i=0}^{\infty} \sum_{j=0}^{i} \frac{\tilde{c}_j(m_1\gamma_1, m_2\gamma_2)\tilde{c}_{i-j}(m_2\gamma_2, m_1\gamma_1)}{2\Gamma\big((n_T n_R - k)m_1\gamma_1 + km_2\gamma_2 + j\gamma_1 + (i-j)\gamma_2\big)} \tag{3.73}$$

$$\Gamma\left(\frac{(n_T n_R-k)m_1\gamma_1+km_2\gamma_2+j\gamma_1+(i-j)\gamma_2}{2}\right)s^{-\frac{(n_T n_R-k)m_1\gamma_1+km_2\gamma_2+j\gamma_1+(i-j)\gamma_2}{2}}$$

Where,

$$\tilde{c}_0(m_1\gamma_1,m_2\gamma_2)=\left[\tilde{b}_0(m_1\gamma_1,m_2\gamma_2)\right]^{n_T n_R-k} \tag{3.74}$$

$$\tilde{c}_0(m_2\gamma_2,m_1\gamma_1)=\left[\tilde{b}_0(m_2\gamma_2,m_1\gamma_1)\right]^{n_T n_R-k} \tag{3.75}$$

$$\tilde{c}_m(m_1\gamma_1,m_2\gamma_2)=\frac{1}{m\tilde{b}_0(m_1\gamma_1,m_2\gamma_2)} \tag{3.76}$$

$$\sum_{l=0}^{m}(l(n_T n_R-k)-m+l)\,\tilde{b}_0(m_1\gamma_1,m_2\gamma_2)\tilde{c}_{m-l}(m_1\gamma_1,m_2\gamma_2)$$

$$\tilde{c}_m(m_2\gamma_2,m_1\gamma_1)=\frac{1}{m\tilde{b}_0(m_2\gamma_2,m_1\gamma_1)}\sum_{l=0}^{m}(l(n_T n_R-k)-m+l)\times \tag{3.77}$$

$$\tilde{b}_0(m_2\gamma_2,m_1\gamma_1)\tilde{c}_{m-l}(m_2\gamma_2,m_1\gamma_1)$$

From equations (3.71) and (3.73),

$$P_{M-PAM}=2\left(1-\frac{1}{M}\right)\sum_{k=0}^{n_T n_R}\binom{n_T n_R}{k}$$

$$\sum_{i=0}^{\infty}\sum_{j=0}^{i}\frac{\tilde{c}_j(m_1\gamma_1,m_2\gamma_2)\tilde{c}_{i-j}(m_2\gamma_2,m_1\gamma_1)}{2\Gamma\left((n_T n_R-k)m_1\gamma_1+km_2\gamma_2+j\gamma_1+(i-j)\gamma_2\right)}\Lambda_{ij}(n_T n_R,M) \tag{3.78}$$

$$\Gamma\left(\frac{(n_T n_R-k)m_1\gamma_1+km_2\gamma_2+j\gamma_1+(i-j)\gamma_2}{2}\right)\left(\frac{\phi\gamma}{n_T^2 n_R}\right)^{-\frac{(n_T n_R-k)m_1\gamma_1+km_2\gamma_2+j\gamma_1+(i-j)\gamma_2}{2}}$$

Where,

$$\Lambda_{ij}(n_T n_R,M)=\frac{1}{\pi}\int_0^{\frac{\pi}{2}}(\sin\theta)^{(n_T n_R-k)m_1\gamma_1+km_2\gamma_2+j\gamma_1+(i-j)\gamma_2}\,d\theta \tag{3.79}$$

$$\Lambda_{ij}(n_T n_R,M)$$
$$=\frac{\Gamma\left[\frac{1}{2}(1-k\mathrm{m}_1\gamma_1+\mathrm{m}_1 n_T n_R\gamma_1+j(\gamma_1-\gamma_2)+i\gamma_2+km_2\gamma_2)\right]}{2\sqrt{\pi}\,\Gamma\left[\frac{1}{2}(2-k\mathrm{m}_1\gamma_1+\mathrm{m}_1 n_T n_R\gamma_1+j(\gamma_1-\gamma_2)+i\gamma_2+km_2\gamma_2)\right]} \tag{3.80}$$

3.1.5 AVERAGE SYMBOL ERROR RATE OF M-QAM FOR MIMO FSO SYSTEM WITH RC SCHEME

The average SER for MQAM can be evaluated as

$$P_{M-QAM} = \xi_1 \int_0^{\pi/2} M_{Y^2}\left(\frac{\phi\bar{\gamma}}{n_T^2 n_R sin^2\theta}\right) d\theta - \xi_2 \int_0^{\pi/4} M_{Y^2}\left(\frac{\phi\bar{\gamma}}{n_T^2 n_R sin^2\theta}\right) d\theta \quad (3.81)$$

Where,

$$\phi = \frac{3}{2(M-1)}, \xi_1 = \frac{4}{\pi}\left(1-\frac{1}{\sqrt{M}}\right), and\ \xi_2 = \frac{4}{\pi}\left(1-\frac{1}{\sqrt{M}}\right)^2 \quad (3.82)$$

And from equation (3.60), we have

$$M_{Y^2}(s) = \sum_{k=0}^{n_T n_R} \binom{n_T n_R}{k} \sum_{i=0}^{\infty}\sum_{j=0}^{i} \frac{\tilde{c}_j(m_1\gamma_1, m_2\gamma_2)\tilde{c}_{i-j}(m_2\gamma_2, m_1\gamma_1)}{2\Gamma\big((n_T n_R - k)m_1\gamma_1 + km_2\gamma_2 + j\gamma_1 + (i-j)\gamma_2\big)}$$
$$\Gamma\left(\frac{(n_T n_R - k)m_1\gamma_1 + km_2\gamma_2 + j\gamma_1 + (i-j)\gamma_2}{2}\right) s^{-\frac{(n_T n_R - k)m_1\gamma_1 + km_2\gamma_2 + j\gamma_1 + (i-j)\gamma_2}{2}} \quad (3.83)$$

Where,

$$\tilde{c}_0(m_1\gamma_1, m_2\gamma_2) = \left[\tilde{b}_0(m_1\gamma_1, m_2\gamma_2)\right]^{n_T n_R - k} \quad (3.84)$$

$$\tilde{c}_0(m_2\gamma_2, m_1\gamma_1) = \left[\tilde{b}_0(m_2\gamma_2, m_1\gamma_1)\right]^{n_T n_R - k} \quad (3.85)$$

$$\tilde{c}_m(m_1\gamma_1, m_2\gamma_2) = \frac{1}{m\tilde{b}_0(m_1\gamma_1, m_2\gamma_2)} \quad (3.86)$$
$$\sum_{l=0}^{m}(l(n_T n_R - k) - m + l)\,\tilde{b}_0(m_1\gamma_1, m_2\gamma_2)\tilde{c}_{m-l}(m_1\gamma_1, m_2\gamma_2)$$

$$\tilde{c}_m(m_2\gamma_2, m_1\gamma_1) = \frac{1}{m\tilde{b}_0(m_2\gamma_2, m_1\gamma_1)}\sum_{l=0}^{m}(l(n_T n_R - k) - m + l) \times \quad (3.87)$$
$$\tilde{b}_0(m_2\gamma_2, m_1\gamma_1)\tilde{c}_{m-l}(m_2\gamma_2, m_1\gamma_1)$$

From equations (3.81) and (3.83),

$$P_{M-QAM} = 4\left(1-\frac{1}{\sqrt{M}}\right)\sum_{k=0}^{n_T n_R}\binom{n_T n_R}{k} \quad (3.88)$$

$$\sum_{i=0}^{\infty}\sum_{j=0}^{i}\frac{\tilde{c}_j(m_1\gamma_1,m_2\gamma_2)\tilde{c}_{i-j}(m_2\gamma_2,m_1\gamma_1)}{2\Gamma\big((n_Tn_R-k)m_1\gamma_1+km_2\gamma_2+j\gamma_1+(i-j)\gamma_2\big)}\Lambda_{ij}(n_Tn_R,M)$$

$$\left(\frac{\phi\bar{\gamma}}{n_T^2n_R}\right)^{-\frac{(n_Tn_R-k)m_1\gamma_1+km_2\gamma_2+j\gamma_1+(i-j)\gamma_2}{2}} -$$

$$4\left(1-\frac{1}{\sqrt{M}}\right)^2\sum_{k=0}^{n_Tn_R}\binom{n_Tn_R}{k}\sum_{i=0}^{\infty}\sum_{j=0}^{i}\frac{\tilde{c}_j(m_1\gamma_1,m_2\gamma_2)\tilde{c}_{i-j}(m_2\gamma_2,m_1\gamma_1)}{2\Gamma\big((n_Tn_R-k)m_1\gamma_1+km_2\gamma_2+j\gamma_1+(i-j)\gamma_2\big)}$$

$$\psi_{ij}(n_Tn_R,M)\left(\frac{\phi\bar{\gamma}}{n_T^2n_R}\right)^{-\frac{(n_Tn_R-k)m_1\gamma_1+km_2\gamma_2+j\gamma_1+(i-j)\gamma_2}{2}}$$

Where,

$$\Lambda_{ij}(n_Tn_R,M)=\frac{1}{\pi}\int_0^{\frac{\pi}{2}}(\sin\theta)^{(n_Tn_R-k)m_1\gamma_1+km_2\gamma_2+j\gamma_1+(i-j)\gamma_2}\,d\theta \tag{3.89}$$

$$\Lambda_{ij}(n_Tn_R,M)=\frac{\Gamma\left[\frac{1}{2}(1-k\mathrm{m}_1\gamma_1+\mathrm{m}_1n_Tn_R\gamma_1+j(\gamma_1-\gamma_2)+i\gamma_2+km_2\gamma_2)\right]}{2\sqrt{\pi}\,\Gamma\left[\frac{1}{2}(2-k\mathrm{m}_1\gamma_1+\mathrm{m}_1n_Tn_R\gamma_1+j(\gamma_1-\gamma_2)+i\gamma_2+km_2\gamma_2)\right]} \tag{3.90}$$

$$\psi_{ij}(n_Tn_R,M)=\frac{1}{\pi}\int_0^{\frac{\pi}{4}}(\sin\theta)^{(n_Tn_R-k)m_1\gamma_1+km_2\gamma_2+j\gamma_1+(i-j)\gamma_2}\,d\theta \tag{3.91}$$

$$\psi_{ij}(n_Tn_R,M)=\frac{2^{\frac{1}{2}(-1+k\mathrm{m}_1\gamma_1-\mathrm{m}_1n_Tn_R\gamma_1-i\gamma_2-km_2\gamma_2+j(-\gamma_1+\gamma_2))}}{\big(\pi(-1-j\gamma_1+k\mathrm{m}_1\gamma_1-\mathrm{m}_1n_Tn_R\gamma_1-i\gamma_2+j\gamma_2-k\mathrm{m2y2})\big)}\times$$

$$e^{-\frac{1}{2}i\pi(1-k\mathrm{m}_1\gamma_1+\mathrm{m}_1n_Tn_R\gamma_1 1+j(\gamma_1-\gamma_2)+i\gamma_2+km_2\gamma_2)}$$

$$\begin{aligned}&2\mathrm{F}1\left[\frac{1}{2},\frac{1}{2}(1-k\mathrm{m}_1\gamma_1+\mathrm{m}_1n_Tn_R\gamma_1+j(\gamma_1-\gamma_2)+i\gamma_2+km_2\gamma_2),\frac{1}{2}(3-k\mathrm{m}_1\gamma_1\right.\\&\qquad\left.+\mathrm{m}_1n_Tn_R\gamma_1+j(\gamma_1-\gamma_2)+i\gamma_2+km_2\gamma_2),\frac{1}{2}\right]\times\end{aligned} \tag{3.92}$$

$$\begin{aligned}&(\cos\left[\frac{1}{2}\pi(-1-k\mathrm{m}_1\gamma_1+\mathrm{m}_1n_Tn_R\gamma_1+j(\gamma_1-\gamma_2)+i\gamma_2+km_2\gamma_2)\right]\\&+i\sin\left[\frac{1}{2}\pi(-1-k\mathrm{m}_1\gamma_1+\mathrm{m}_1n_Tn_R\gamma_1+j(\gamma_1-\gamma_2)+i\gamma_2+km_2\gamma_2)\right])\end{aligned}$$

3.1.6 AVERAGE SYMBOL ERROR RATE OF MPSK FOR SISO FSO SYSTEM

Let $X = I^2$ represents a random variable which depends on the channel fading.

Based on the series expansion of the double GG PDF (3.6), we can derive the PDF of X as

$$f_I(I) = \sum_{l=0}^{\infty} (a_l(m_1\gamma_1, m_2\gamma_2) I^{l\gamma_1+m_1\gamma_1-1} + a_l(m_1\gamma_1, m_2\gamma_2) I^{l\gamma_1+m_1\gamma_1-1}) \tag{3.93}$$

Now, changing the random variable

$$X = I^2 \tag{3.94}$$

$$I = \sqrt{X} \tag{3.95}$$

$$f_X(x) = |J| f_I(I) \tag{3.96}$$

$$|J| = \frac{\partial x}{\partial I} \tag{3.97}$$

$$\frac{\partial x}{\partial I} = \frac{1}{2\sqrt{I}} \tag{3.98}$$

$$f_x(X) = \sum_{l=0}^{\infty} (a_l(m_1\gamma_1, m_2\gamma_2) x^{\frac{l\gamma_1+m_1\gamma_1}{2}-1} + a_l(m_1\gamma_1, m_2\gamma_2) x^{\frac{l\gamma_1+m_1\gamma_1}{2}-1}) \tag{3.99}$$

with the help of [23, Eq. 3.478(1)], the MGF of X is derived by

$$M_X(s) = \sum_{l=0}^{\infty} b_l(m_1\gamma_1, m_2\gamma_2) s^{-\frac{l\gamma_1+m_1\gamma_1}{2}} + \sum_{l=0}^{\infty} b_l(m_2\gamma_2, m_1\gamma_1) s^{-\frac{l\gamma_2+m_2\gamma_2}{2}} \tag{3.100}$$

Where,

$$b_l(m_1\gamma_1, m_2\gamma_2) = \frac{a_l(m_1\gamma_1, m_2\gamma_2)}{2} \Gamma\left(\frac{l\gamma_1 + m_1\gamma_1}{2}\right) \tag{3.101}$$

$$b_l(m_2\gamma_2, m_1\gamma_1) = \frac{a_l(m_1\gamma_1, m_2\gamma_2)}{2} \Gamma\left(\frac{l\gamma_1 + m_1\gamma_1}{2}\right) \tag{3.102}$$

The average SER of subcarrier MPSK can be evaluated as

$$P_{MPSK} = \frac{1}{\pi} \int_0^{\frac{(M-1)\pi}{M}} M_X\left(\frac{\phi\bar{\gamma}}{sin^2\theta}\right) d\theta \tag{3.103}$$

Where,

$$\phi = sin^2\left(\frac{\pi}{M}\right) \tag{3.104}$$

From equations (3.100) and (3.103),

$$P_{MPSK} = \sum_{l=0}^{\infty} b_l(m_1\gamma_1, m_2\gamma_2)\Lambda(m_1\gamma_1)(\phi\gamma)^{-\frac{l\gamma_1+m_1\gamma_1}{2}} + \sum_{l=0}^{\infty} b_l(m_2\gamma_2, m_1\gamma_1)\Lambda(m_2\gamma_2)(\phi\gamma)^{-\frac{l\gamma_2+m_2\gamma_2}{2}} \tag{3.105}$$

Where,

$$\Lambda(m_1\gamma_1) = \frac{1}{\pi}\int_0^{\frac{(M-1)\pi}{M}} (sin\,\theta)^{l\gamma_1+m_1\gamma_1}\,d\theta \tag{3.106}$$

$$\Lambda(m_1\gamma_1) = \frac{\Gamma\left[\frac{1}{2}(1+(l+m_1)\gamma_1)\right]}{2\sqrt{\pi}\Gamma\left[1+\frac{1}{2}(l+\mathrm{m}_1)\gamma_1\right]} + \frac{\cos\left[\frac{\pi}{M}\right]2F1\left[\frac{1}{2},\frac{1}{2}-\frac{1}{2}(l+m_1)\gamma_1,\frac{3}{2},\cos\left[\frac{\pi}{M}\right]^2\right]}{\pi} \tag{3.107}$$

and

$$\Lambda(m_2\gamma_2) = \frac{1}{\pi}\int_0^{\frac{(M-1)\pi}{M}} (sin\,\theta)^{l\gamma_2+m_2\gamma_2}\,d\theta \tag{3.108}$$

$$\Lambda(m_2\gamma_2) = \frac{\Gamma\left[\frac{1}{2}(1+(l+m_2)\gamma_2)\right]}{2\sqrt{\pi}\Gamma\left[1+\frac{1}{2}(l+\mathrm{m}_2)\gamma_2\right]} + \frac{\cos\left[\frac{\pi}{M}\right]2F1\left[\frac{1}{2},\frac{1}{2}-\frac{1}{2}(l+m_2)\gamma_2,\frac{3}{2},\cos\left[\frac{\pi}{M}\right]^2\right]}{\pi} \tag{3.109}$$

3.1.7 AVERAGE SYMBOL ERROR RATE OF M-PAM FOR SISO FSO SYSTEM

The average SER of M-PAM can be evaluated as

$$P_{M-PAM} = \frac{2}{\pi}\left(1-\frac{1}{M}\right)\int_0^{\frac{\pi}{2}} M_X\left(\frac{\phi\bar{\gamma}}{sin^2\,\theta}\right)d\theta \tag{3.110}$$

Where,

$$\phi = \frac{3}{(M^2-1)} \tag{3.111}$$

And from equation (3.100), we have

$$M_X(s) = \sum_{l=0}^{\infty} b_l(m_1\gamma_1, m_2\gamma_2)s^{-\frac{l\gamma_1+m_1\gamma_1}{2}} + \sum_{l=0}^{\infty} b_l(m_2\gamma_2, m_1\gamma_1)s^{-\frac{l\gamma_2+m_2\gamma_2}{2}} \tag{3.112}$$

Where,

$$b_l(m_1\gamma_1, m_2\gamma_2) = \frac{a_l(m_1\gamma_1, m_2\gamma_2)}{2}\Gamma\left(\frac{l\gamma_1 + m_1\gamma_1}{2}\right) \tag{3.113}$$

$$b_l(m_2\gamma_2, m_1\gamma_1) = \frac{a_l(m_1\gamma_1, m_2\gamma_2)}{2}\Gamma\left(\frac{l\gamma_1 + m_1\gamma_1}{2}\right) \tag{3.114}$$

From equations (3.110) and (3.112),

$$P_{M-PAM} = 2\left(1-\frac{1}{M}\right)\sum_{l=0}^{\infty} b_l(m_1\gamma_1, m_2\gamma_2)\Lambda(m_1\gamma_1)(\phi\bar{\gamma})^{-\frac{l\gamma_1+m_1\gamma_1}{2}} + \sum_{l=0}^{\infty} b_l(m_2\gamma_2, m_1\gamma_1)\Lambda(m_2\gamma_2)(\phi\bar{\gamma})^{-\frac{l\gamma_2+m_2\gamma_2}{2}} \tag{3.115}$$

Where,

$$\Lambda(m_1\gamma_1) = \frac{1}{\pi}\int_0^{\frac{\pi}{2}} (\sin\theta)^{l\gamma_1+m_1\gamma_1}\, d\theta \tag{3.116}$$

$$\Lambda(m_1\gamma_1) = \frac{\Gamma\left[\frac{1}{2}(1+(l+\mathrm{m}_1)\gamma_1)\right]}{2\sqrt{\pi}\Gamma\left[1+\frac{1}{2}(l+\mathrm{m}_1)\gamma_1\right]} \tag{3.117}$$

and

$$\Lambda(m_2\gamma_2) = \frac{1}{\pi}\int_0^{\frac{\pi}{2}} (\sin\theta)^{l\gamma_2+m_2\gamma_2}\, d\theta \tag{3.118}$$

$$\Lambda(m_2\gamma_2) = \frac{\Gamma\left[\frac{1}{2}(1+(l+\mathrm{m}_2)\gamma_2)\right]}{2\sqrt{\pi}\Gamma\left[1+\frac{1}{2}(l+\mathrm{m}_2)\gamma_2\right]} \tag{3.119}$$

3.1.8 AVERAGE SYMBOL ERROR RATE OF M-QAM FOR SISO FSO SYSTEM

The average SER of M-QAM can be evaluated as

$$P_{M-QAM} = \xi_1\int_0^{\pi/2} M_X\left(\frac{\phi\bar{\gamma}}{\sin^2\theta}\right)d\theta - \xi_2\int_0^{\pi/4} M_X\left(\frac{\phi\bar{\gamma}}{\sin^2\theta}\right)d\theta \tag{3.120}$$

Where,

$$\phi = \frac{3}{2(M-1)}, \xi_1 = \frac{4}{\pi}\left(1-\frac{1}{\sqrt{M}}\right), and\ \xi_2 = \frac{4}{\pi}\left(1-\frac{1}{\sqrt{M}}\right)^2 \tag{3.121}$$

And from equation (3.100), we have

$$M_X(s) = \sum_{l=0}^{\infty} b_l(m_1\gamma_1, m_2\gamma_2) s^{-\frac{l\gamma_1+m_1\gamma_1}{2}} + \sum_{l=0}^{\infty} b_l(m_2\gamma_2, m_1\gamma_1) s^{-\frac{l\gamma_2+m_2\gamma_2}{2}} \quad (3.122)$$

Where,

$$b_l(m_1\gamma_1, m_2\gamma_2) = \frac{a_l(m_1\gamma_1, m_2\gamma_2)}{2} \Gamma\left(\frac{l\gamma_1 + m_1\gamma_1}{2}\right) \quad (3.123)$$

$$b_l(m_2\gamma_2, m_1\gamma_1) = \frac{a_l(m_1\gamma_1, m_2\gamma_2)}{2} \Gamma\left(\frac{l\gamma_1 + m_1\gamma_1}{2}\right) \quad (3.124)$$

From equations (3.120) and (3.122),

$$\begin{aligned} P_{M-QAM} = {} & 4\left(1 - \frac{1}{\sqrt{M}}\right) \sum_{l=0}^{\infty} b_l(m_1\gamma_1, m_2\gamma_2) \Lambda(m_1\gamma_1)(\phi\bar{\gamma})^{-\frac{l\gamma_1+m_1\gamma_1}{2}} \\ & + \sum_{l=0}^{\infty} b_l(m_2\gamma_2, m_1\gamma_1) \Lambda(m_2\gamma_2)(\phi\bar{\gamma})^{-\frac{l\gamma_2+m_2\gamma_2}{2}} - \\ & 4\left(1 - \frac{1}{\sqrt{M}}\right)^2 \sum_{l=0}^{\infty} b_l(m_1\gamma_1, m_2\gamma_2) \Psi(m_1\gamma_1)(\phi\bar{\gamma})^{-\frac{l\gamma_1+m_1\gamma_1}{2}} \\ & + \sum_{l=0}^{\infty} b_l(m_2\gamma_2, m_1\gamma_1) \Psi(m_2\gamma_2)(\phi\bar{\gamma})^{-\frac{l\gamma_2+m_2\gamma_2}{2}} \end{aligned} \quad (3.125)$$

Where,

$$\Lambda(m_1\gamma_1) = \frac{1}{\pi} \int_0^{\frac{\pi}{2}} (\sin\theta)^{l\gamma_1+m_1\gamma_1} \, d\theta \quad (3.126)$$

$$\Lambda(m_1\gamma_1) = \frac{\Gamma\left[\frac{1}{2}(1 + (l + \mathrm{m}_1)\gamma_1)\right]}{2\sqrt{\pi}\Gamma\left[1 + \frac{1}{2}(l + \mathrm{m}_1)\gamma_1\right]} \quad (3.127)$$

and

$$\Lambda(m_2\gamma_2) = \frac{1}{\pi} \int_0^{\frac{\pi}{2}} (\sin\theta)^{l\gamma_2+m_2\gamma_2} \, d\theta \quad (3.128)$$

$$\Lambda(m_2\gamma_2) = \frac{\Gamma\left[\frac{1}{2}(1 + (l + \mathrm{m}_2)\gamma_2)\right]}{2\sqrt{\pi}\Gamma\left[1 + \frac{1}{2}(l + \mathrm{m}_2)\gamma_2\right]} \quad (3.129)$$

and,

$$\Psi(m_1\gamma_1) = \frac{1}{\pi} \int_0^{\frac{\pi}{4}} (\sin\theta)^{l\gamma_1+m_1\gamma_1} \, d\theta \quad (3.130)$$

$$\Psi(m_1\gamma_1) = \frac{i2^{\frac{1}{2}(-1-l\gamma_1-\mathrm{m}_1\gamma_1)}e^{-\frac{1}{2}i\pi(1+l\gamma_1+\mathrm{m}_1\gamma_1)}(\mathrm{Cos}[\frac{1}{2}(l+\mathrm{m}_1)\pi\gamma_1]}{\pi(1+l\gamma_1+\mathrm{m}_1\gamma_1)}$$

$$+\left(\frac{i\mathrm{Cos}\left[\frac{1}{2}\pi(-1+l\gamma_1+\mathrm{m}_1\gamma_1)\right])}{\pi(1+l\gamma_1+\mathrm{m}_1\gamma_1)}\right)\times \tag{3.131}$$

$$\mathrm{Hypergeometric2F1}\left[\frac{1}{2},\frac{1}{2}(1+(l+\mathrm{m}_1)\gamma_1),\frac{1}{2}(3+(l+\mathrm{m}_1)\gamma_1),\frac{1}{2}\right]$$

and

$$\Psi(m_2\gamma_2) = \frac{1}{\pi}\int_0^{\frac{\pi}{4}}(sin\,\theta)^{l\gamma_2+m_2\gamma_2}\,d\theta \tag{3.132}$$

$$\Psi(m_2\gamma_2) = \frac{i2^{\frac{1}{2}(-1-l\gamma_2-\mathrm{m}_2\gamma_2)}e^{-\frac{1}{2}i\pi(1+l\gamma_2+\mathrm{m}_2\gamma_2)}(\mathrm{Cos}[\frac{1}{2}(l+\mathrm{m}_2)\pi\gamma_2]}{\pi(1+l\gamma_2+\mathrm{m}_2\gamma_2)}$$

$$+\left(\frac{i\mathrm{Cos}\left[\frac{1}{2}\pi(-1+l\gamma_2+\mathrm{m}_2\gamma_2)\right])}{\pi(1+l\gamma_2+\mathrm{m}_2\gamma_2)}\right)\times \tag{3.133}$$

$$\mathrm{Hypergeometric2F1}\left[\frac{1}{2},\frac{1}{2}(1+(l+\mathrm{m}_2)\gamma_2),\frac{1}{2}(3+(l+\mathrm{m}_2)\gamma_2),\frac{1}{2}\right]$$

CHAPTER 4

SIMULATION RESULT AND ANALYSIS

4.1 RESULT AND ANALYSIS

4.1.1 THE AVERAGE SER OF SUBCARRIER MPSK FOR A MIMO FSO SYSTEM WITH THE RC SCHEME

The average SER of subcarrier MPSK for a MIMO FSO system with the RC scheme has been derived. The expression is mentioned below:

$$P_{M,\ RC} = \sum_{k=0}^{n_T n_R} \binom{n_T n_R}{k} \sum_{i=0}^{\infty} \sum_{j=0}^{i} \frac{\tilde{c}_j(m_1\gamma_1, m_2\gamma_2)\tilde{c}_{i-j}(m_2\gamma_2, m_1\gamma_1)}{2\Gamma\big((n_T n_R - k)m_1\gamma_1 + km_2\gamma_2 + j\gamma_1 + (i-j)\gamma_2\big)} \Lambda_{ij}(n_T n_R, M)\Gamma\left(\frac{(n_T n_R - k)m_1\gamma_1 + km_2\gamma_2 + j\gamma_1 + (i-j)\gamma_2}{2}\right) \left(\frac{\mathcal{k}\bar{\gamma}}{n_T^2 n_R sin^2\theta}\right)^{-\frac{(n_T n_R - k)m_1\gamma_1 + km_2\gamma_2 + j\gamma_1 + (i-j)\gamma_2}{2}} \quad (4.1)$$

Where,

$$\Lambda_{ij}(n_T n_R, M) = \frac{\sqrt{\pi}\Gamma\left(\frac{1 + (n_T n_R - k)m_1\gamma_1 + j\gamma_1 + km_2\gamma_2 + (i-j)\gamma_2}{2}\right)}{2\Gamma\left(1 + \frac{(n_T n_R - k)m_1\gamma_1 + j\gamma_1 + km_2\gamma_2 + (i-j)\gamma_2}{2}\right)} - \cos\left(\frac{M-1}{M}\pi\right) 2F1\left[\frac{1}{2}, \frac{1 - (n_T n_R - k)m_1\gamma_1 - j\gamma_1 - km_2\gamma_2 - (i-j)\gamma_2}{2}; \frac{3}{2}; cos^2\left(\frac{M-}{M}\right.\right. \quad (4.2)$$

$$\mathcal{k} = sin^2\left(\frac{\pi}{M}\right) \quad (4.3)$$

n_T and n_R are the number of lasers and number of photodetectors respectively.

γ_i> 0 and m_i> 0.5 are the parameters of the generalized gamma distribution.

4.1.2 AVERAGE SER OF SUBCARRIER MPSK FOR MIMO FSO SYSTEM

The average SER of subcarrier MPSK for MIMO FSO system with the RC scheme has been derived. The expression is mentioned below:

$$P_{M,\ RC} = \sum_{k=0}^{n_T n_R} \binom{n_T n_R}{k} \sum_{i=0}^{\infty} \sum_{j=0}^{i} \frac{\tilde{c}_j(m_1\gamma_1, m_2\gamma_2)\tilde{c}_{i-j}(m_2\gamma_2, m_1\gamma_1)}{2\Gamma\big((n_T n_R - k)m_1\gamma_1 + km_2\gamma_2 + j\gamma_1 + (i-j)\gamma_2\big)}$$

$$\Lambda_{ij}(n_T n_R, M)\Gamma\left(\frac{(n_T n_R - k)m_1\gamma_1 + km_2\gamma_2 + j\gamma_1 + (i-j)\gamma_2}{2}\right) \tag{4.4}$$

$$\left(\frac{\hbar\bar{\gamma}}{n_T^2 n_R sin^2\theta}\right)^{-\frac{(n_T n_R - k)m_1\gamma_1 + km_2\gamma_2 + j\gamma_1 + (i-j)\gamma_2}{2}}$$

Where,

$$\Lambda_{ij}(n_T n_R, M) = \frac{\sqrt{\pi}\Gamma\left(\frac{1 + (n_T n_R - k)m_1\gamma_1 + j\gamma_1 + km_2\gamma_2 + (i-j)\gamma_2}{2}\right)}{2\Gamma\left(1 + \frac{(n_T n_R - k)m_1\gamma_1 + j\gamma_1 + km_2\gamma_2 + (i-j)\gamma_2}{2}\right)} - \cos\left(\frac{M-1}{M}\pi\right) \tag{4.5}$$

$$2F1\left[\frac{1}{2}, \frac{1 - (n_T n_R - k)m_1\gamma_1 - j\gamma_1 - km_2\gamma_2 - (i-j)\gamma_2}{2}; \frac{3}{2}; cos^2\left(\frac{M-1}{M}\pi\right)\right]$$

$$\hbar = sin^2\left(\frac{\pi}{M}\right) \tag{4.6}$$

n_T and n_R are the number of lasers and number of photodetectors respectively.

$\gamma_i > 0$ and $m_i > 0.5$ are the parameters of the generalized gamma distribution.

4.1.3 AVERAGE SER OF M-PAM FOR MIMO FSO SYSTEM

The expression for SER of M-PAM for MIMO FSO system with the RC scheme is mentioned below

$$P_{M-PAM} = 2\left(1 - \frac{1}{M}\right) \sum_{k=0}^{n_T n_R} \binom{n_T n_R}{k}$$

$$\sum_{i=0}^{\infty} \sum_{j=0}^{i} \frac{\tilde{c}_j(m_1\gamma_1, m_2\gamma_2)\tilde{c}_{i-j}(m_2\gamma_2, m_1\gamma_1)}{2\Gamma\big((n_T n_R - k)m_1\gamma_1 + km_2\gamma_2 + j\gamma_1 + (i-j)\gamma_2\big)} \Lambda_{ij}(n_T n_R, M) \tag{4.7}$$

$$\Gamma\left(\frac{(n_T n_R - k)m_1\gamma_1 + km_2\gamma_2 + j\gamma_1 + (i-j)\gamma_2}{2}\right)\left(\frac{\phi\gamma}{n_T^2 n_R}\right)^{-\frac{(n_T n_R - k)m_1\gamma_1 + km_2\gamma_2 + j\gamma_1 + (}{2}}$$

Where,

$$\Lambda_{ij}(n_T n_R, M) = \frac{\Gamma\left[\frac{1}{2}(1 - k\mathrm{m}_1\gamma_1 + \mathrm{m}_1 n_T n_R \gamma_1 + j(\gamma_1 - \gamma_2) + i\gamma_2 + km_2\gamma_2)\right]}{2\sqrt{\pi}\,\Gamma\left[\frac{1}{2}(2 - k\mathrm{m}_1\gamma_1 + \mathrm{m}_1 n_T n_R \gamma_1 + j(\gamma_1 - \gamma_2) + i\gamma_2 + km_2\gamma_2)\right]} \tag{4.8}$$

$$\phi = \frac{3}{(M^2 - 1)} \tag{4.9}$$

4.1.4 AVERAGE SER OF M-QAM FOR MIMO FSO SYSTEM

The expression for SER of M-QAM for MIMO FSO system with the RC scheme is mentioned below

$$P_{M-QAM} = 4\left(1 - \frac{1}{\sqrt{M}}\right)\sum_{k=0}^{n_T n_R}\binom{n_T n_R}{k} \sum_{i=0}^{\infty}\sum_{j=0}^{i}\frac{\tilde{c}_j(m_1\gamma_1, m_2\gamma_2)\tilde{c}_{i-j}(m_2\gamma_2, m_1\gamma_1)}{2\Gamma\big((n_T n_R - k)m_1\gamma_1 + km_2\gamma_2 + j\gamma_1 + (i-j)\gamma_2\big)}\Lambda_{ij}(n_T n_R, M) \left(\frac{\phi\bar{\gamma}}{n_T^2 n_R}\right)^{-\frac{(n_T n_R - k)m_1\gamma_1 + km_2\gamma_2 + j\gamma_1 + (i-j)\gamma_2}{2}} - 4\left(1 - \frac{1}{\sqrt{M}}\right)^2 \sum_{k=0}^{n_T n_R}\binom{n_T n_R}{k}\sum_{i=0}^{\infty}\sum_{j=0}^{i}\frac{\tilde{c}_j(m_1\gamma_1, m_2\gamma_2)\tilde{c}_{i-j}(m_2\gamma_2, m_1\gamma_1)}{2\Gamma\big((n_T n_R - k)m_1\gamma_1 + km_2\gamma_2 + j\gamma_1 + (i-j)\gamma_2\big)} \psi_{ij}(n_T n_R, M)\left(\frac{\phi\bar{\gamma}}{n_T^2 n_R}\right)^{-\frac{(n_T n_R - k)m_1\gamma_1 + km_2\gamma_2 + j\gamma_1 + (i-j)\gamma_2}{2}} \tag{4.10}$$

Where,

$$\Lambda_{ij}(n_T n_R, M) = \frac{\Gamma\left[\frac{1}{2}(1 - k\mathrm{m}_1\gamma_1 + \mathrm{m}_1 n_T n_R \gamma_1 + j(\gamma_1 - \gamma_2) + i\gamma_2 + km_2\gamma_2)\right]}{2\sqrt{\pi}\,\Gamma\left[\frac{1}{2}(2 - k\mathrm{m}_1\gamma_1 + \mathrm{m}_1 n_T n_R \gamma_1 + j(\gamma_1 - \gamma_2) + i\gamma_2 + km_2\gamma_2)\right]} \tag{4.11}$$

$$\psi_{ij}(n_T n_R, M) = \frac{2^{\frac{1}{2}(-1 + k\mathrm{m}_1\gamma_1 - \mathrm{m}_1 n_T n_R \gamma_1 - i\gamma_2 - km_2\gamma_2 + j(-\gamma_1 + \gamma_2))}}{\big(\pi(-1 - j\gamma_1 + k\mathrm{m}_1\gamma_1 - \mathrm{m}_1 n_T n_R \gamma_1 - i\gamma_2 + j\gamma_2 - k\mathrm{m}2\mathrm{y}2)\big)} \times e^{-\frac{1}{2}i\pi(1 - k\mathrm{m}_1\gamma_1 + \mathrm{m}_1 n_T n_R \gamma_1 1 + j(\gamma_1 - \gamma_2) + i\gamma_2 + km_2\gamma_2)} \tag{4.12}$$

$$2F1\left[\frac{1}{2},\frac{1}{2}(1-k\mathrm{m}_1\gamma_1+\mathrm{m}_1 n_T n_R \gamma_1+j(\gamma_1-\gamma_2)+i\gamma_2+km_2\gamma_2),\frac{1}{2}(3 - k\mathrm{m}_1\gamma_1+\mathrm{m}_1 n_T n_R \gamma_1+j(\gamma_1-\gamma_2)+i\gamma_2+km_2\gamma_2),\frac{1}{2}\right]$$

$$\times$$

$$(\cos\left[\frac{1}{2}\pi(-1-k\mathrm{m}_1\gamma_1+\mathrm{m}_1 n_T n_R \gamma_1+j(\gamma_1-\gamma_2)+i\gamma_2+km_2\gamma_2)\right]$$

$$+ i\, \sin\left[\frac{1}{2}\pi(-1-k\mathrm{m}_1\gamma_1+\mathrm{m}_1 n_T n_R \gamma_1+j(\gamma_1-\gamma_2)+i\gamma_2+km_2\gamma_2)\right])$$

$$\phi = \frac{3}{2(M-1)} \tag{4.13}$$

4.1.5 AVERAGE SER OF SUBCARRIER MPSK FOR SISO FSO SYSTEM

The expression for SER of subcarrier MPSK for SISO FSO system is mentioned below

$$P_{MPSK} = \sum_{l=0}^{\infty} b_l(m_1\gamma_1, m_2\gamma_2)\Lambda(m_1\gamma_1)(\phi\gamma)^{-\frac{l\gamma_1+m_1\gamma_1}{2}} + \sum_{l=0}^{\infty} b_l(m_2\gamma_2, m_1\gamma_1)\Lambda(m_2\gamma_2)(\phi\gamma)^{-\frac{l\gamma_2+m_2\gamma_2}{2}} \tag{4.14}$$

Where,

$$\Lambda(m_1\gamma_1) = \frac{\Gamma\left[\frac{1}{2}(1+(l+m_1)\gamma_1)\right]}{2\sqrt{\pi}\Gamma\left[1+\frac{1}{2}(l+\mathrm{m}_1)\gamma_1\right]} + \frac{\cos\left[\frac{\pi}{M}\right]2F1\left[\frac{1}{2},\frac{1}{2}-\frac{1}{2}(l+m_1)\gamma_1,\frac{3}{2},\cos\left[\frac{\pi}{M}\right]^2\right]}{\pi} \tag{4.15}$$

and

$$\Lambda(m_2\gamma_2) = \frac{\Gamma\left[\frac{1}{2}(1+(l+m_2)\gamma_2)\right]}{2\sqrt{\pi}\Gamma\left[1+\frac{1}{2}(l+\mathrm{m}_2)\gamma_2\right]} + \frac{\cos\left[\frac{\pi}{M}\right]2F1\left[\frac{1}{2},\frac{1}{2}-\frac{1}{2}(l+m_2)\gamma_2,\frac{3}{2},\cos\left[\frac{\pi}{M}\right]^2\right]}{\pi} \tag{4.16}$$

4.1.6 AVERAGE SER OF SUBCARRIER M-PAM FOR SISO FSO SYSTEM

The expression for SER of M-PAM for SISO FSO system is mentioned below

$$P_{M-PAM} = 2\left(1-\frac{1}{M}\right)\sum_{l=0}^{\infty} b_l(m_1\gamma_1, m_2\gamma_2)\Lambda(m_1\gamma_1)(\phi\bar{\gamma})^{-\frac{l\gamma_1+m_1\gamma_1}{2}} + \sum_{l=0}^{\infty} b_l(m_2\gamma_2, m_1\gamma_1)\Lambda(m_2\gamma_2)(\phi\bar{\gamma})^{-\frac{l\gamma_2+m_2\gamma_2}{2}} \tag{4.17}$$

Where,

$$\Lambda(m_1\gamma_1) = \frac{\Gamma\left[\frac{1}{2}(1+(l+\mathrm{m}_1)\gamma_1)\right]}{2\sqrt{\pi}\Gamma\left[1+\frac{1}{2}(l+\mathrm{m}_1)\gamma_1\right]} \tag{4.18}$$

and

$$\Lambda(m_2\gamma_2) = \frac{\Gamma\left[\frac{1}{2}(1+(l+\mathrm{m}_2)\gamma_2)\right]}{2\sqrt{\pi}\Gamma\left[1+\frac{1}{2}(l+\mathrm{m}_2)\gamma_2\right]} \tag{4.19}$$

4.1.7 AVERAGE SER OF SUBCARRIER M-QAM FOR SISO FSO SYSTEM

The expression for SER of M-QAM for SISO FSO system is mentioned below

$$\begin{aligned} P_{M-PAM} = {} & 4\left(1-\frac{1}{\sqrt{M}}\right)\sum_{l=0}^{\infty} b_l(m_1\gamma_1, m_2\gamma_2)\Lambda(m_1\gamma_1)(\phi\bar{\gamma})^{-\frac{l\gamma_1+m_1\gamma_1}{2}} \\ & + \sum_{l=0}^{\infty} b_l(m_2\gamma_2, m_1\gamma_1)\Lambda(m_2\gamma_2)(\phi\bar{\gamma})^{-\frac{l\gamma_2+m_2\gamma_2}{2}} - \\ & 4\left(1-\frac{1}{\sqrt{M}}\right)^2\sum_{l=0}^{\infty} b_l(m_1\gamma_1, m_2\gamma_2)\Psi(m_1\gamma_1)(\phi\bar{\gamma})^{-\frac{l\gamma_1+m_1\gamma_1}{2}} \\ & + \sum_{l=0}^{\infty} b_l(m_2\gamma_2, m_1\gamma_1)\Psi(m_2\gamma_2)(\phi\bar{\gamma})^{-\frac{l\gamma_2+m_2\gamma_2}{2}} \end{aligned} \tag{4.20}$$

Where,

$$\Lambda(m_1\gamma_1) = \frac{\Gamma\left[\frac{1}{2}(1+(l+\mathrm{m}_1)\gamma_1)\right]}{2\sqrt{\pi}\Gamma\left[1+\frac{1}{2}(l+\mathrm{m}_1)\gamma_1\right]} \tag{4.21}$$

and

$$\Lambda(m_2\gamma_2) = \frac{\Gamma\left[\frac{1}{2}(1+(l+\mathrm{m}_2)\gamma_2)\right]}{2\sqrt{\pi}\Gamma\left[1+\frac{1}{2}(l+\mathrm{m}_2)\gamma_2\right]} \tag{4.22}$$

and,

$$\Psi(m_1\gamma_1) = \frac{i2^{\frac{1}{2}(-1-l\gamma_1-\mathrm{m}_1\gamma_1)}e^{-\frac{1}{2}i\pi(1+l\gamma_1+\mathrm{m}_1\gamma_1)}(\mathrm{Cos}[\frac{1}{2}(l+\mathrm{m}_1)\pi\gamma_1]}{\pi(1+l\gamma_1+\mathrm{m}_1\gamma_1)}$$

$$+\left(\frac{i\mathrm{Cos}\left[\frac{1}{2}\pi(-1+l\gamma_1+\mathrm{m}_1\gamma_1)\right])}{\pi(1+l\gamma_1+\mathrm{m}_1\gamma_1)}\right)\times \tag{4.23}$$

$$\mathrm{Hypergeometric2F1}\left[\frac{1}{2},\frac{1}{2}(1+(l+\mathrm{m}_1)\gamma_1),\frac{1}{2}(3+(l+\mathrm{m}_1)\gamma_1),\frac{1}{2}\right]$$

and

$$\Psi(m_2\gamma_2) = \frac{i2^{\frac{1}{2}(-1-l\gamma_2-\mathrm{m}_2\gamma_2)}e^{-\frac{1}{2}i\pi(1+l\gamma_2+\mathrm{m}_2\gamma_2)}(\mathrm{Cos}[\frac{1}{2}(l+\mathrm{m}_2)\pi\gamma_2]}{\pi(1+l\gamma_2+\mathrm{m}_2\gamma_2)}$$

$$+\left(\frac{i\mathrm{Cos}\left[\frac{1}{2}\pi(-1+l\gamma_2+\mathrm{m}_2\gamma_2)\right])}{\pi(1+l\gamma_2+\mathrm{m}_2\gamma_2)}\right)\times \tag{4.24}$$

$$\mathrm{Hypergeometric2F1}\left[\frac{1}{2},\frac{1}{2}(1+(l+\mathrm{m}_2)\gamma_2),\frac{1}{2}(3+(l+\mathrm{m}_2)\gamma_2),\frac{1}{2}\right]$$

4.1.8 PLOT OF BER vs SNR FOR MIMO MPSK:

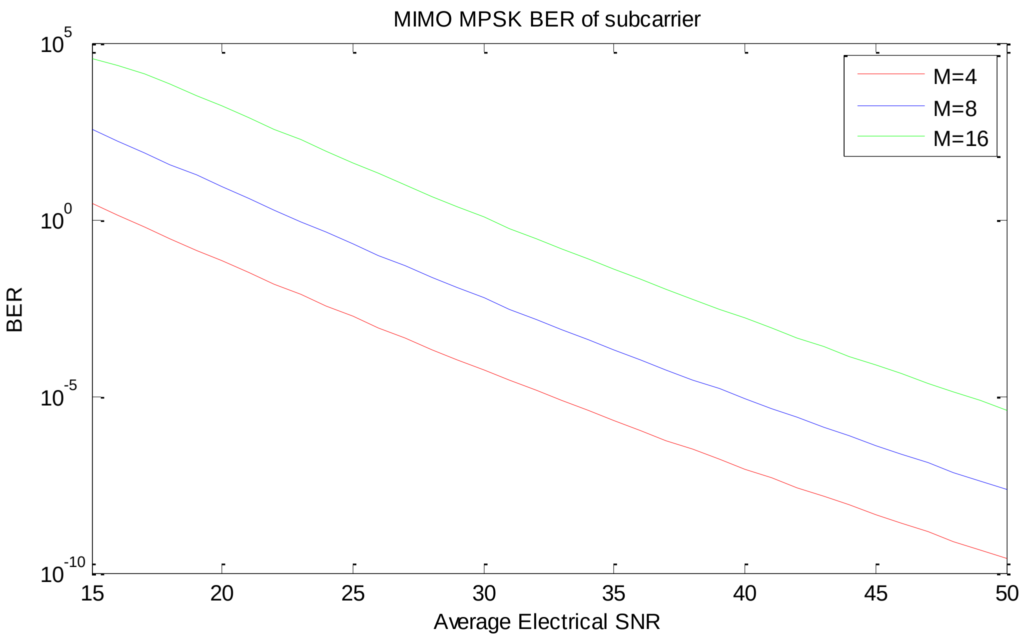

Fig 4.1 BER vs SNR for MIMO MPSK under moderate turbulence condition.

The plot 4.1 shows the BER of subcarrier MPSK for MIMO FSO system over double GG fading for different values of M, under moderate turbulence condition with the parameters $m_1 = 2.65, \gamma_1 = 0.9135, \Omega_1 = 0.9836, m_2 = 0.85, \gamma_2 = 1.4358, \Omega_2 = 1.1745, n_T =$

$2, n_R = 2$. It is overserved from the plot that BER decreases on increasing the SNR for a particular value of M and the BER increases on increasing the value of M for a particular SNR.

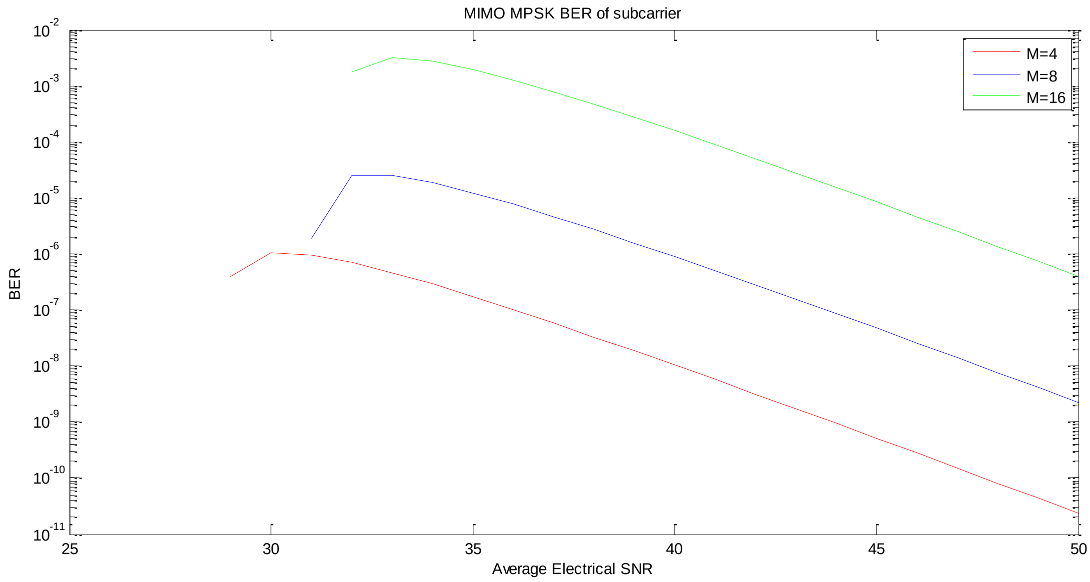

Fig 4.2 BER vs SNR for MIMO MPSK under strong turbulence condition.

The plot 4.2 shows the BER of subcarrier MPSK for MIMO FSO system over double GG fading for different values of M, under strong turbulence condition with the parameters $m_1 = 0.5, \gamma_1 = 1.8621, \Omega_1 = 1.5074, m_2 = 1.8, \gamma_2 = 0.7638, \Omega_2 = 0.928, n_T = 2, n_R = 2$. It is overserved from the plot that BER decreases on increasing the SNR for a particular value of M and the BER increases on increasing the value of M for a particular SNR.

4.1.9 PLOT OF BER vs SNR FOR MIMO M-PAM:

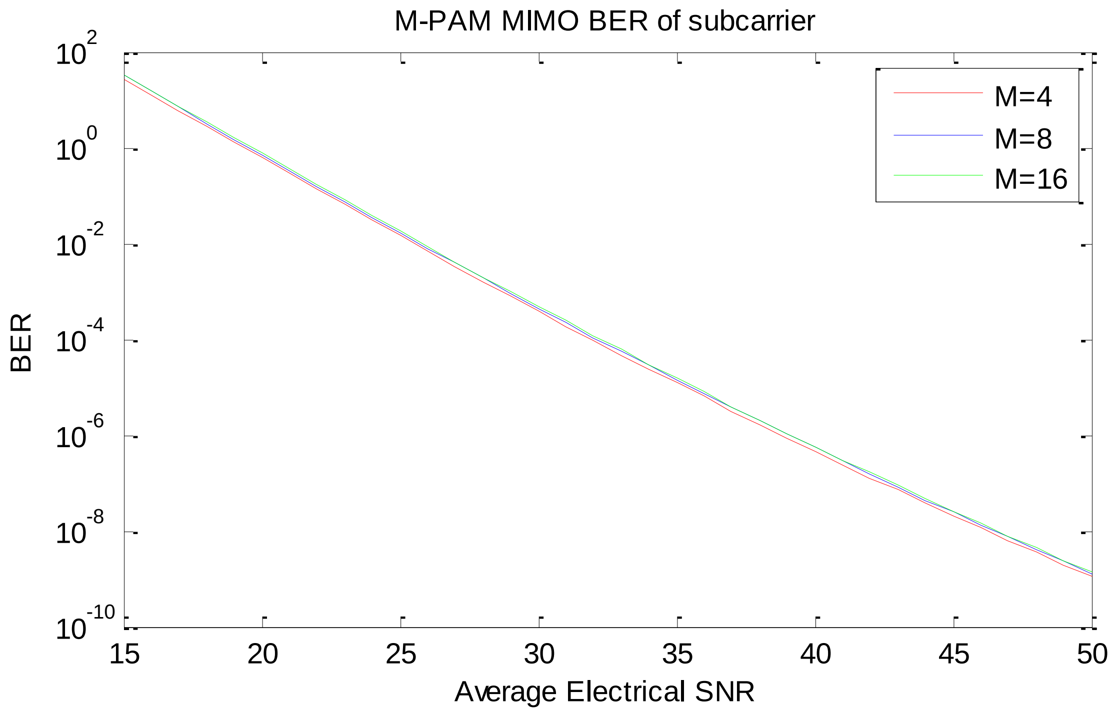

Fig 4.3 BER vs SNR for MIMO M-PAM under moderate turbulence condition.

The plot 4.3 shows the BER of M-PAM for MIMO FSO system over double GG fading for different values of M, under moderate turbulence condition with the parameters $m_1 = 2.65, \gamma_1 = 0.9135, \Omega_1 = 0.9836, m_2 = 0.85, \gamma_2 = 1.4358, \Omega_2 = 1.1745, n_T = 2, n_R = 2$. It is overserved from the plot that BER decreases on increasing the SNR for a particular value of M and the BER increases on increasing the value of M for a particular SNR.

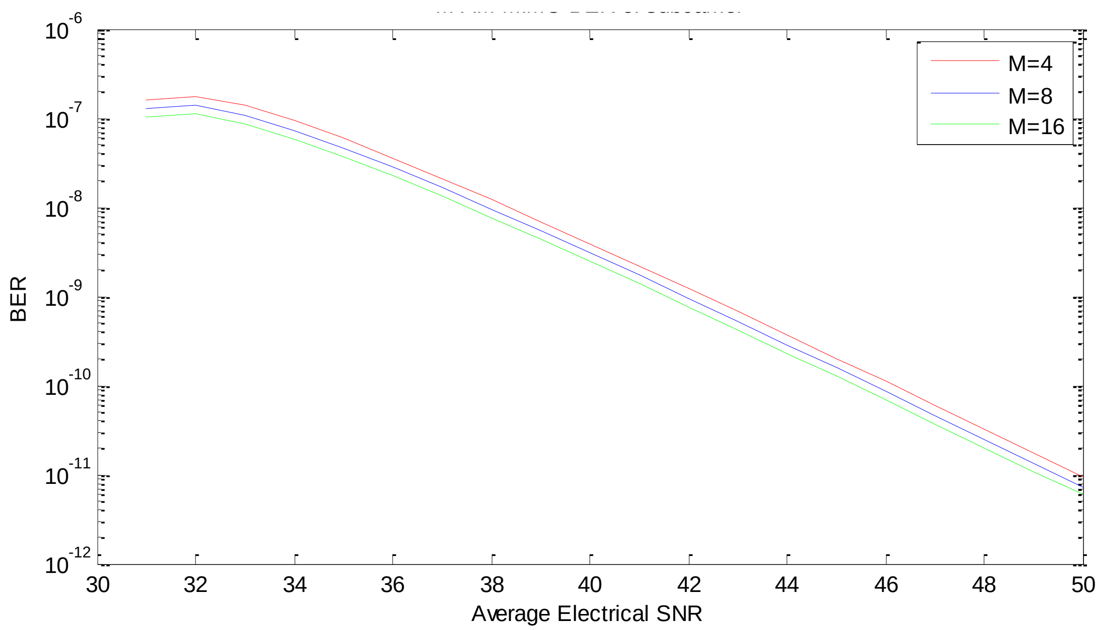

Fig 4.4 BER vs SNR for MIMO M-PAM under strong turbulence condition.

The plot 4.4 shows the BER of M-PAM for MIMO FSO system over double GG fading for different values of M, under strong turbulence condition with the parameters $m_1 = 0.5, \gamma_1 = 1.8621, \Omega_1 = 1.5074, m_2 = 1.8, \gamma_2 = 0.7638, \Omega_2 = 0.928, n_T = 2, n_R = 2$. It is overserved from the plot that BER decreases on increasing the SNR for a particular value of M and the BER increases on increasing the value of M for a particular SNR.

4.1.10 PLOT OF BER vs SNR FOR MIMO M-QAM:

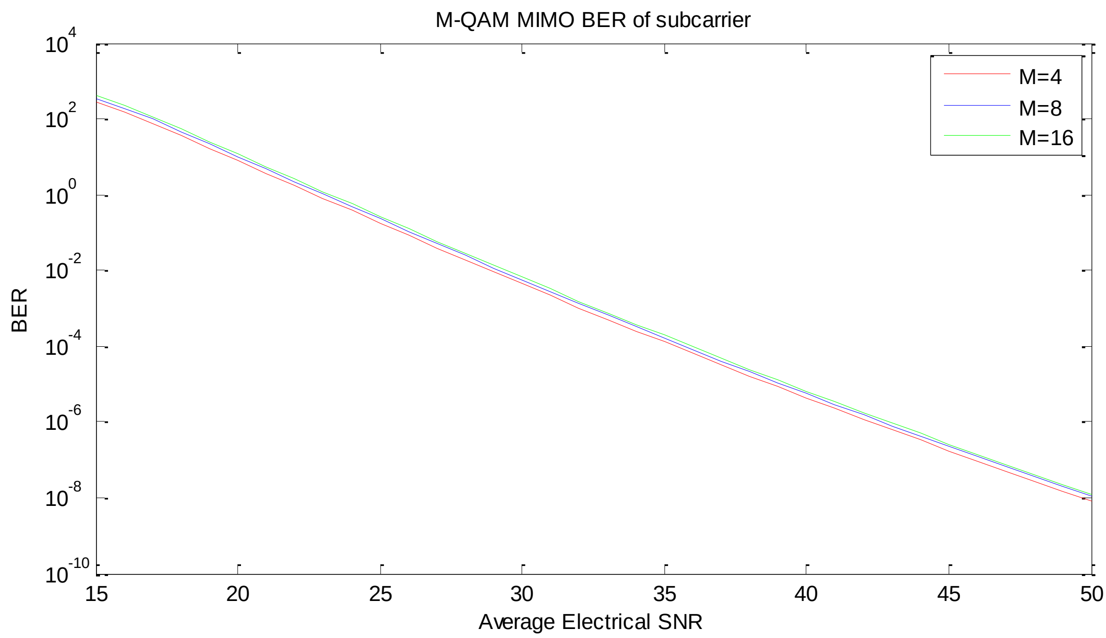

Fig 4.5 BER vs SNR for MIMO M-QAM under moderate turbulence condition.

The plot 4.5 shows the BER of M-QAM for MIMO FSO system over double GG fading for different values of M, under moderate turbulence condition with the parameters $m_1 = 2.65, \gamma_1 = 0.9135, \Omega_1 = 0.9836, m_2 = 0.85, \gamma_2 = 1.4358, \Omega_2 = 1.1745, n_T = 2, n_R = 2$. It is overserved from the plot that BER decreases on increasing the SNR for a particular value of M and the BER increases on increasing the value of M for a particular SNR.

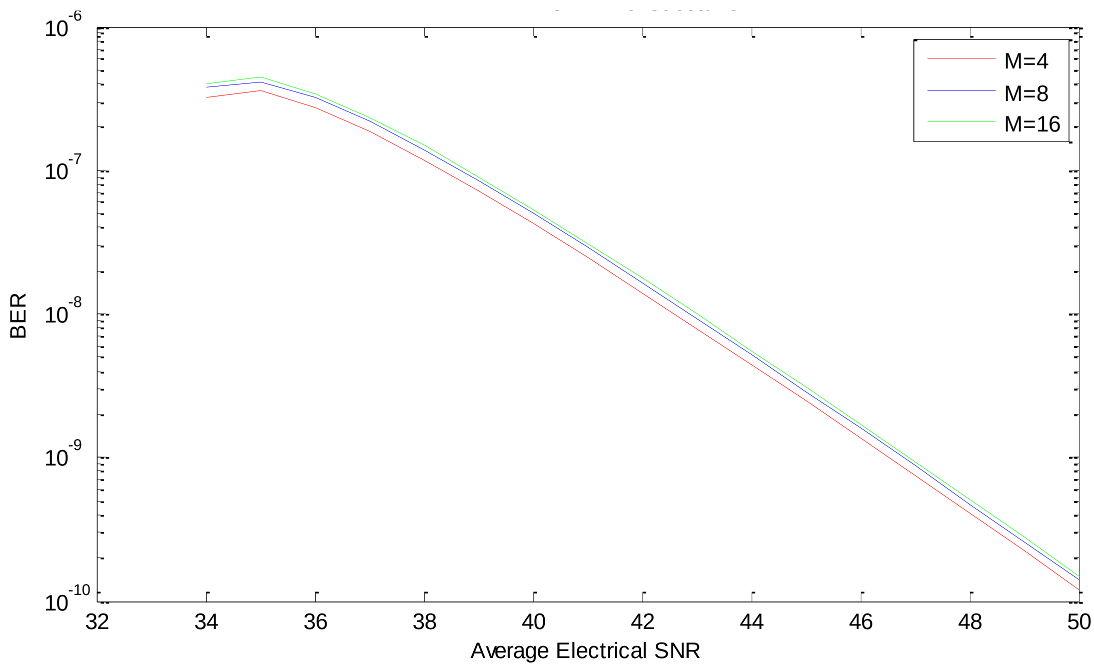

Fig 4.6 BER vs SNR for MIMO M-QAM under strong turbulence condition.

The plot 4.6 shows the BER of M-QAM for MIMO FSO system over double GG fading for different values of M, under strong turbulence condition with the parameters $m_1 = 0.5, \gamma_1 = 1.8621, \Omega_1 = 1.5074, m_2 = 1.8, \gamma_2 = 0.7638, \Omega_2 = 0.928, n_T = 2, n_R = 2$. It is overserved from the plot that BER decreases on increasing the SNR for a particular value of M and the BER increases on increasing the value of M for a particular SNR.

4.1.11 PLOT OF BER vs SNR FOR SISO MPSK:

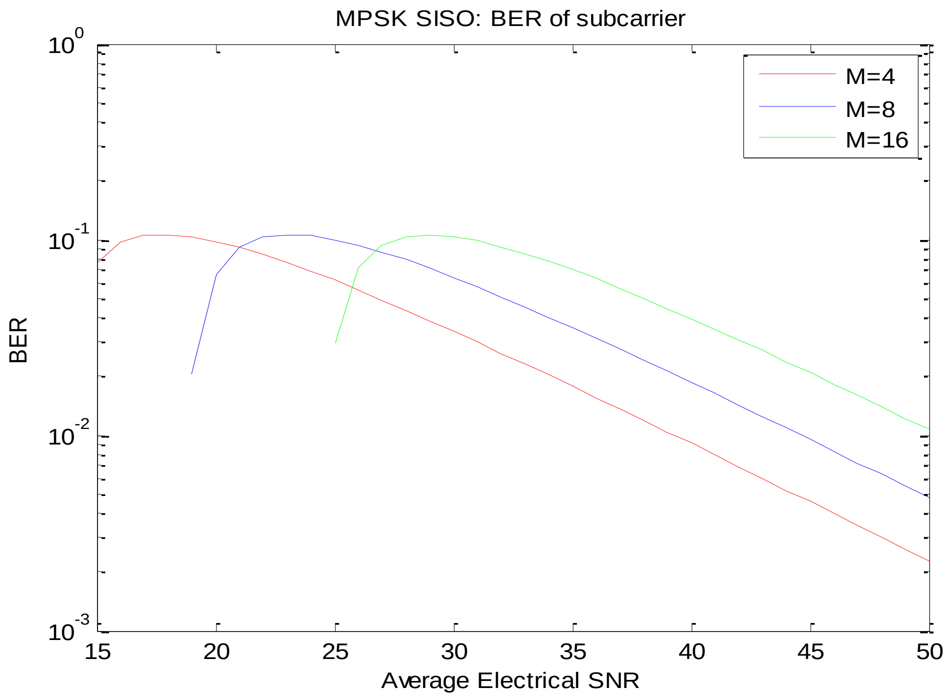

Fig 4.7 BER vs SNR for SISO MPSK under moderate turbulence condition.

The plot 4.9 shows the BER of subcarrier MPSK for SISO FSO system over double GG fading for different values of M, under moderate turbulence condition with the parameters $m_1 = 2.65, \gamma_1 = 0.9135, \Omega_1 = 0.9836, m_2 = 0.85, \gamma_2 = 1.4358, \Omega_2 = 1.1745$. It is overserved from the plot that BER decreases on increasing the SNR for a particular value of M and the BER increases on increasing the value of M for a particular SNR.

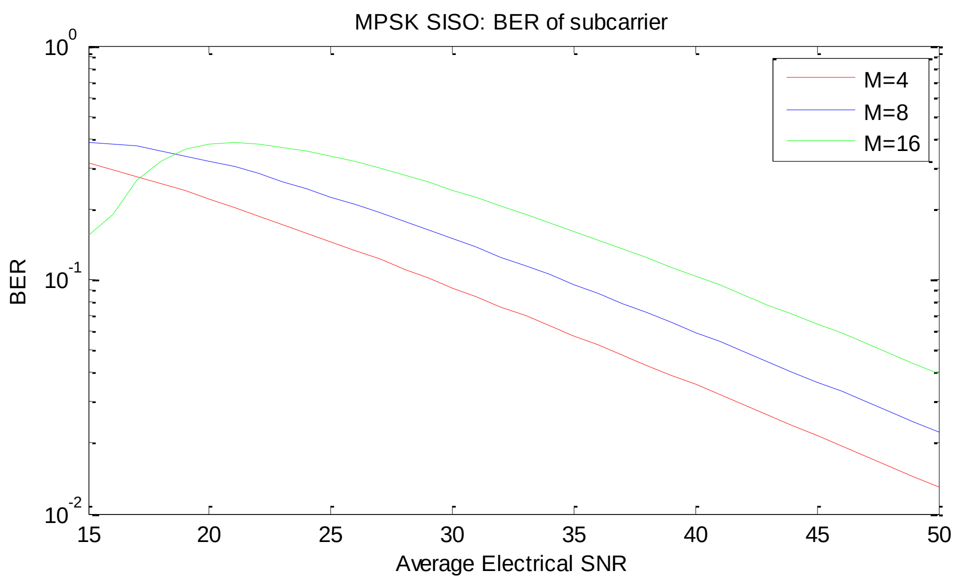

Fig 4.8 BER vs SNR for SISO MPSK under strong turbulence condition.

The plot 4.10 shows the BER of subcarrier MPSK for SISO FSO system over double GG fading for different values of M, under strong turbulence condition with the parameters $m_1 = 0.5, \gamma_1 = 1.8621, \Omega_1 = 1.5074, m_2 = 1.8, \gamma_2 = 0.7638, \Omega_2 = 0.928$. It is overserved from the plot that BER decreases on increasing the SNR for a particular value of M and the BER increases on increasing the value of M for a particular SNR.

4.1.12 PLOT OF BER vs SNR FOR SISO M-PAM:

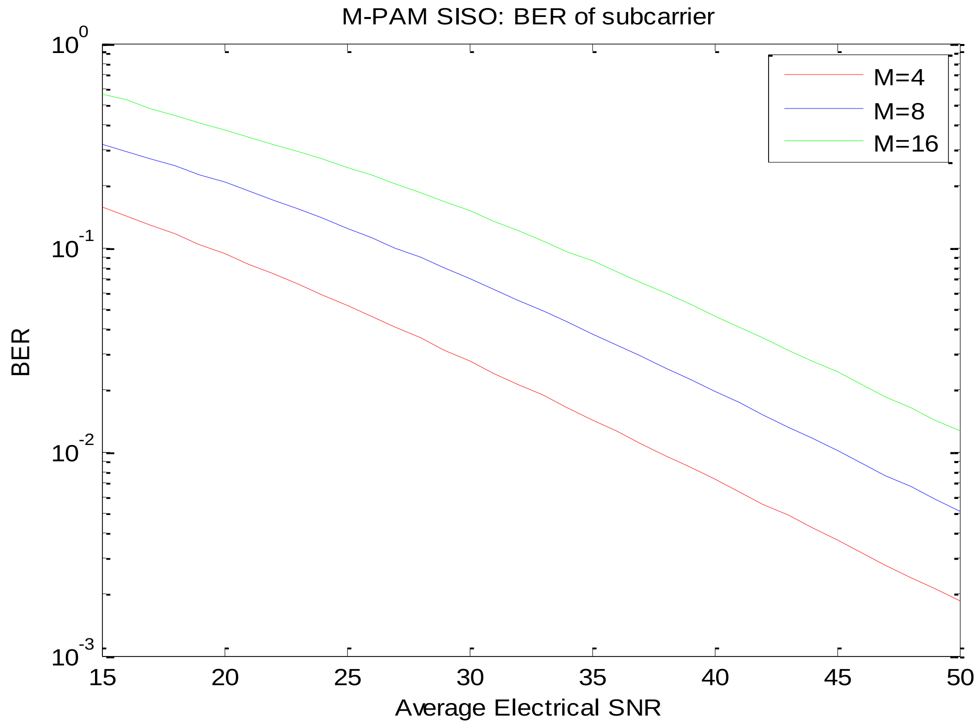

Fig 4.9 BER vs SNR for SISO M-PAM under moderate turbulence condition.

The plot 4.11 shows the BER of M-PAM for SISO FSO system over double GG fading for different values of M, under moderate turbulence condition with the parameters $m_1 = 2.65, \gamma_1 = 0.9135, \Omega_1 = 0.9836, m_2 = 0.85, \gamma_2 = 1.4358, \Omega_2 = 1.1745$. It is overserved from the plot that BER decreases on increasing the SNR for a particular value of M and the BER increases on increasing the value of M for a particular SNR.

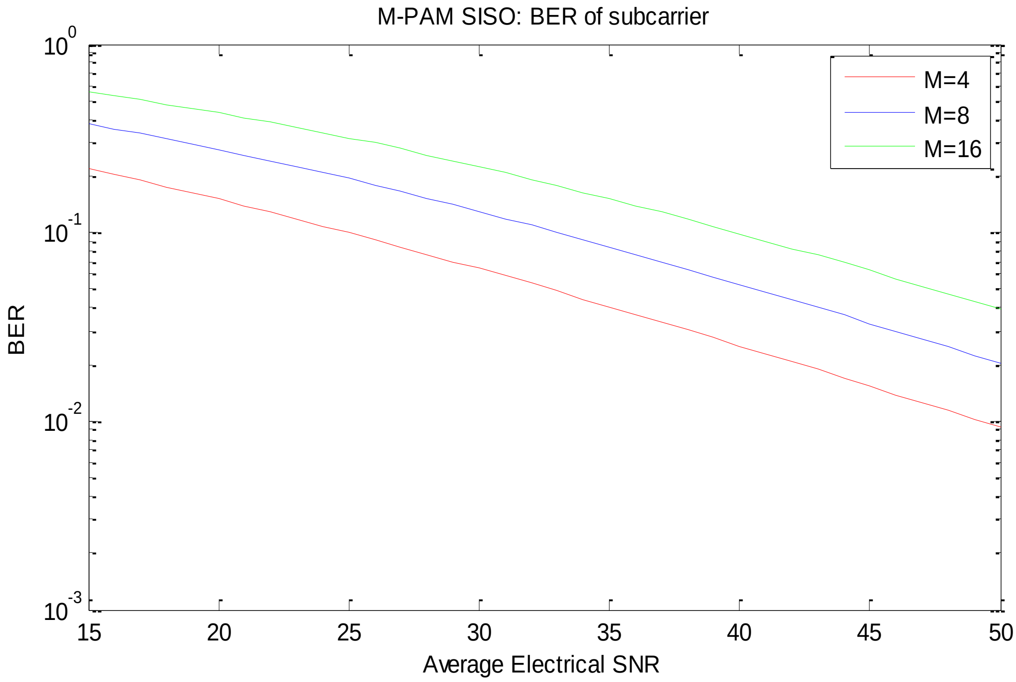

Fig 4.10 BER vs SNR for SISO M-PAM under strong turbulence condition.

The plot 4.12 shows the BER of M-PAM for SISO FSO system over double GG fading for different values of M, under strong turbulence condition with the parameters $m_1 = 0.5, \gamma_1 = 1.8621, \Omega_1 = 1.5074, m_2 = 1.8, \gamma_2 = 0.7638, \Omega_2 = 0.928$. It is overserved from the plot that BER decreases on increasing the SNR for a particular value of M and the BER increases on increasing the value of M for a particular SNR.

4.1.13 PLOT OF BER vs SNR FOR SISO M-QAM:

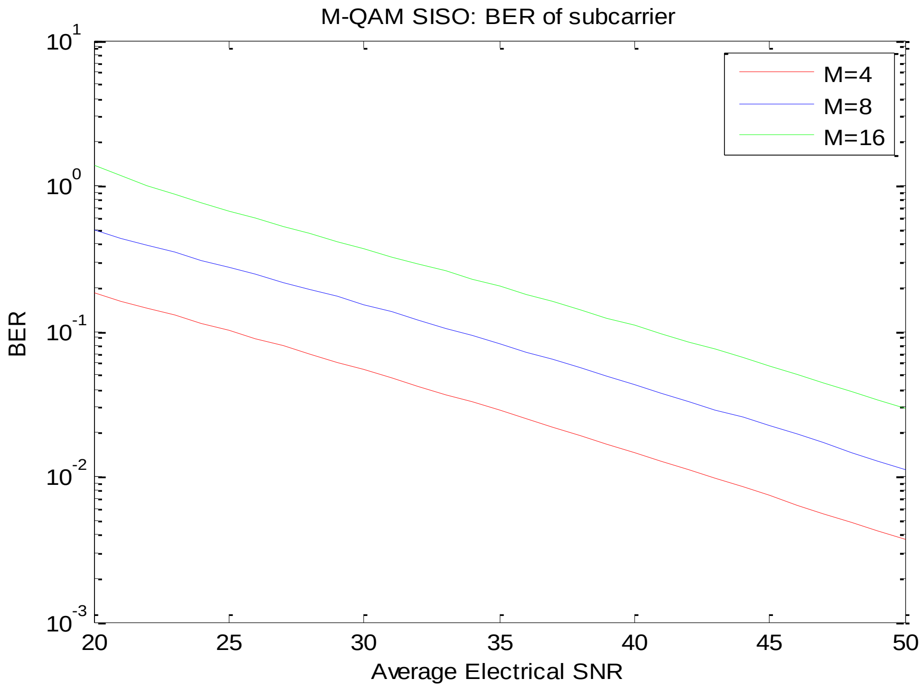

Fig 4.11 BER vs SNR for SISO M-QAM under moderate turbulence condition.

The plot 4.13 shows the BER of M-QAM for SISO FSO system over double GG fading for different values of M, under moderate turbulence condition with the parameters $m_1 = 2.65, \gamma_1 = 0.9135, \Omega_1 = 0.9836, m_2 = 0.85, \gamma_2 = 1.4358, \Omega_2 = 1.1745$. It is overserved from the plot that BER decreases on increasing the SNR for a particular value of M and the BER increases on increasing the value of M for a particular SNR.

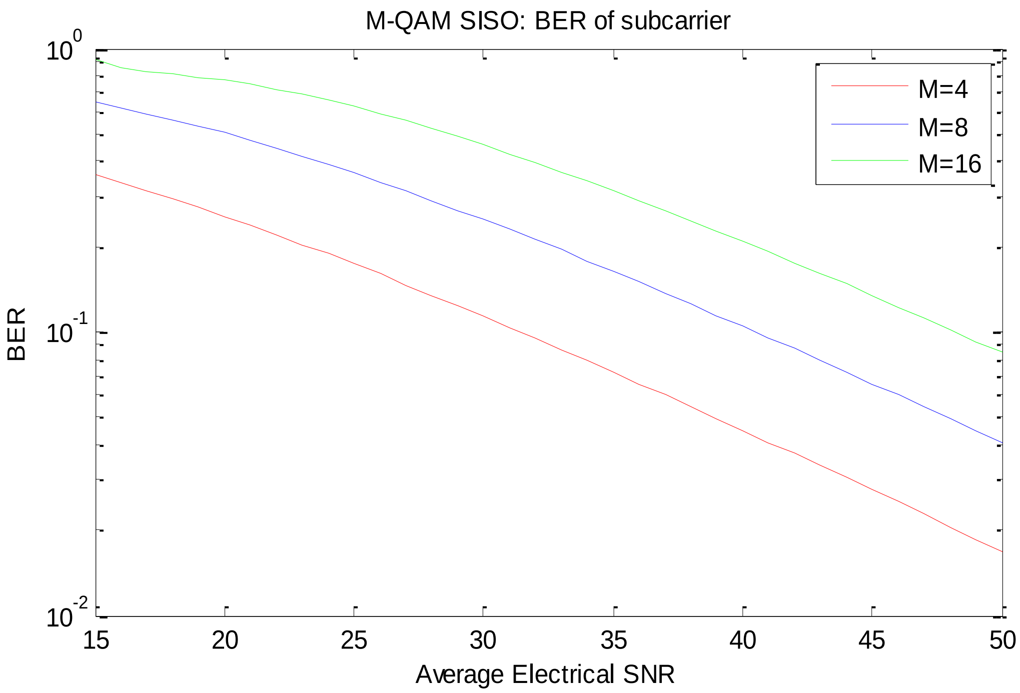

Fig 4.12 BER vs SNR for SISO M-QAM under strong turbulence condition

.

The plot 4.14 shows the BER of M-QAM for SISO FSO system over double GG fading for different values of M, under strong turbulence condition with the parameters $m_1 = 0.5, \gamma_1 = 1.8621, \Omega_1 = 1.5074, m_2 = 1.8, \gamma_2 = 0.7638, \Omega_2 = 0.928$. It is overserved from the plot that BER decreases on increasing the SNR for a particular value of M and the BER increases on increasing the value of M for a particular SNR.

CHAPTER 5

CONCLUSION

REFERENCES

1. Yi, X., Yao, M. and Wang, X., 2017. MIMO FSO communication using subcarrier intensity modulation over double generalized gamma fading. *Optics Communications*, *382*, pp.64-72.
2. Kashani, M.A., Uysal, M. and Kavehrad, M., 2015. A novel statistical channel model for turbulence-induced fading in free-space optical systems. *Journal of Lightwave Technology*, *33*(11), pp.2303-2312.
3. Liu, H., Liao, R., Wei, Z., Hou, Z. and Qiao, Y., 2015. BER analysis of a hybrid modulation scheme based on PPM and MSK subcarrier intensity modulation. *IEEE Photonics Journal*, *7*(4), pp.1-10.
4. Giri, R.K. and Patnaik, B., 2019. Bit error rate performance analysis of hybrid subcarrier intensity modulation-based FSO with spatial diversity in various weather conditions. *Journal of Optical Communications*, *40*(3), pp.307-314.
5. AlQuwaiee, H., Ansari, I.S. and Alouini, M.S., 2016. On the maximum and minimum of double generalized gamma variates with applications to the performance of free-space optical communication systems. *IEEE Transactions on Vehicular Technology*, *65*(11), pp.8822-8831.
6. Kashani, M.A., Uysal, M. and Kavehrad, M., 2015, June. On the performance of MIMO FSO communications over double generalized gamma fading channels. In *2015 IEEE International Conference on Communications (ICC)* (pp. 5144-5149). IEEE.
7. Aminikashani, M., Kavehrad, M. and Gu, W., 2016, February. Error performance analysis of FSO links with equal gain diversity receivers over double generalized gamma fading channels. In *Broadband Access Communication Technologies X* (Vol. 9772, p. 97720R). International Society for Optics and Photonics.
8. Jagadeesh, V.K., Palliyembil, V., Muthuchidambaranathan, P. and Bui, F.M., 2015. Free space optical communication using subcarrier intensity modulation through generalized turbulence channel with pointing error. *Microwave and Optical Technology Letters*, *57*(8), pp.1958-1961.
9. Bhatnagar, M.R. and Ghassemlooy, Z., 2016. Performance analysis of gamma–gamma fading FSO MIMO links with pointing errors. *Journal of Lightwave technology*, *34*(9), pp.2158-2169.

10. Li, J., Liu, J.Q. and Taylor, D.P., 2007. Optical communication using subcarrier PSK intensity modulation through atmospheric turbulence channels.
11. Kaur, P., Jain, V.K. and Kar, S., 2015. Performance analysis of free space optical links using multi-input multi-output and aperture averaging in presence of turbulence and various weather conditions. *IET Communications*, *9*(8), pp.1104-1109.
12. Saeed, R.A. and Abbas, E.B., 2018, August. Performance Evaluation of MIMO FSO Communication with Gamma-Gamma Turbulence Channel using Diversity Techniques. In *2018 International Conference on Computer, Control, Electrical, and Electronics Engineering (ICCCEEE)* (pp. 1-5). IEEE.
13. Johnsi, A.A. and Saminadan, V., 2013, April. Performance of diversity combining techniques for fso-mimo system. In *2013 International Conference on Communication and Signal Processing* (pp. 479-483). IEEE.
14. Saber, M.J. and Keshavarz, A., 2018, May. On performance of adaptive subcarrier intensity modulation over generalized FSO links. In *Electrical Engineering (ICEE), Iranian Conference on* (pp. 358-361). IEEE.
15. Sadiku, M.N., Musa, S.M. and Nelatury, S.R., 2016. Free space optical communications: An overview. *European scientific journal*, *12*(9).
16. Vellakudiyan, J., Muthuchidambaranathan, P., Bui, F.M. and Palliyembil, V., 2015. Performance of a subcarrier intensity modulated differential phase-shift keying over generalized turbulence channel. *AEU-International Journal of Electronics and Communications*, *69*(11), pp.1569-1573.
17. Dabiri, M.T., Sadough, S.M.S. and Khalighi, M.A., 2017. FSO channel estimation for OOK modulation with APD receiver over atmospheric turbulence and pointing errors. *Optics Communications*, *402*, pp.577-584.
18. Kaur, G., Singh, H. and Sappal, A.S., 2017. Free space optical using different modulation techniques—a review. *International Journal of Engineering Trends and Technology (IJETT)*, *43*(2).
19. Popoola, W.O. and Ghassemlooy, Z., 2009. BPSK subcarrier intensity modulated free-space optical communications in atmospheric turbulence. *Journal of Lightwave technology*, *27*(8), pp.967-973.
20. Prabu, K. and Kumar, D.S., 2015. BER analysis for BPSK based SIM–FSO communication system over strong atmospheric turbulence with spatial diversity and pointing errors. *Wireless Personal Communications*, *81*(3), pp.1143-1157.

21. Chatzidiamantis, N.D., Karagiannidis, G.K., Kriezis, E.E. and Matthaiou, M., 2011, June. Diversity combining in hybrid RF/FSO systems with PSK modulation. In *2011 IEEE International Conference on Communications (ICC)* (pp. 1-6). IEEE.
22. Sasiela, R.J., 2007, May. Electromagnetic wave propagation in turbulence: evaluation and application of Mellin transforms. SPIE.
23. Kilbas, A.A., 2004. *H-transforms: Theory and Applications*. CRC Press.
24. Gradshteyn, I.S. and Ryzhik, I.M., 2014. *Table of integrals, series, and products*. Academic press.
25. Ting Jiang and Lin Zhao ,2019. Performance Improvement for Mixed RF–FSO Communication System by Adopting Hybrid Subcarrier Intensity Modulation. *Article in MDPI Appl. Sci. 2019, pp 9, 3724-3724.*
26. Marvin K. Simon and Mohamed-Slim Alouini , *Digital Communication over Fading Channels*
27. Willebrand, H.A. and Ghuman, B.S., 2001. Fiber optics without fiber. *IEEE spectrum*, *38*(8), pp.40-45.
28. Khalighi, M.A. and Uysal, M., 2014. Survey on free space optical communication: A communication theory perspective. *IEEE communications surveys & tutorials*, *16*(4), pp.2231-2258.
29. Anbarasi, K., Hemanth, C. and Sangeetha, R.G., 2017. A review on channel models in free space optical communication systems. *Optics & Laser Technology*, *97*, pp.161-171.
30. Navidpour, S.M., Uysal, M. and Kavehrad, M., 2007. BER performance of free-space optical transmission with spatial diversity. *IEEE Transactions on wireless communications*, *6*(8), pp.2813-2819.
31. Kaushal, H. and Kaddoum, G., 2015. Free space optical communication: challenges and mitigation techniques. *arXiv preprint arXiv:1506.04836*.
32. McCartney, E.J., 1976. Optics of the atmosphere: scattering by molecules and particles. *New York, John Wiley and Sons, Inc., 1976. 421 p.*
33. M. A. Esmail, H. Fathallah and M. Alouini, "Analysis of fog effects on terrestrial Free Space optical communication links," *2016 IEEE International Conference on Communications Workshops (ICC)*, Kuala Lumpur, 2016, pp. 151-156.
34. Nadeem, F., Kvicera, V., Awan, M.S., Leitgeb, E., Muhammad, S.S. and Kandus, G., 2009. Weather effects on hybrid FSO/RF communication link. *IEEE journal on selected areas in communications*, *27*(9), pp.1687-1697.

35. Leitgeb, E., Plank, T., Awan, M.S., Brandl, P., Popoola, W., Ghassemlooy, Z., Ozek, F. and Wittig, M., 2010, June. Analysis and evaluation of optimum wavelengths for free-space optical transceivers. In *2010 12th International Conference on Transparent Optical Networks* (pp. 1-7). IEEE.
36. Popoola, W.O., 2009. *Subcarrier intensity modulated free-space optical communication systems* (Doctoral dissertation, Northumbria University).
37. Chan, V.W., 2006. Free-space optical communications. *Journal of Lightwave technology*, *24*(12), pp.4750-4762.